Department of Justice
2016-DN-BX-0188
Final Report

Novel Concept for Fingerprint Analysis

Principal Investigator:
Dr. Jan Halamek
Assistant Professor
Department of Chemistry, University at Albany, State University of New York
1400 Washington Ave
Albany, NY 12222
Phone: (518) 442-4645
Fax: (518) 442-3462 (Chemistry)
E-mail: jhalamek@albany.edu
https://www.halameklab.com/

Recipient Organization
The Research Foundation of SUNY, University at Albany
Office for Sponsored Programs, MSC 312
1400 Washington Avenue
Albany, New York 12222
RF # 1138922-1-77915
DUNS – 152652822
EIN Number – 14-1368361

Submitting Official
Christine McCrary
Research Administrator, Pre-Award and Compliance Svcs.
University at Albany, 1400 Washington Avenue, Albany, NY 12222
cmccrary@albany.edu

Signature: 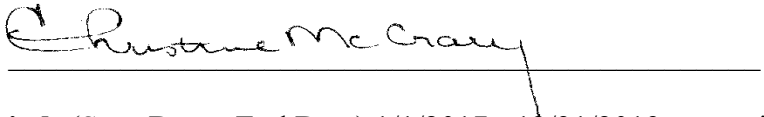

Grant Period: (Start Date - End Date) 1/1/2017 - 12/31/2019, extension to 12/31/2020
Reporting Period End Date: December 31, 2020
Report Term: Semi-Annual
Submission Date: December 31, 2020
Final Report: Yes __X__ No ____

Final Report

I. ACCOMPLISHMENTS

Major Goals of the Project

The ultimate goal of the presented research is the successful development of the fundamental and practical aspects of the biochemical characterization of fingerprint (sweat) content based on its dependence on the fingerprint originator's physical attributes and lifestyle habits. The proposed concept is expected to be robust enough to be used in a variety of circumstances as well as versatile enough to be adapted for different small molecules. The systems will also function with a high degree of selectivity and sensitivity in order to minimize potential errors. The main areas of focus are (I) identify and quantify individual or pools of amino acids and metabolites that would constitute valid determinants of the personal attributes (ethnicity) and indirect personal characteristics (effect of food intake – vegetarian/omnivore or effect of drug consumption) of the fingerprint originator, (II) design and optimize the bioaffinity-based assay protocols for the determination of originator characteristics based on targets identified by mass spectrometry (MS) and evaluate the relevant cascade systems using authentic sweat and fingerprint samples, and (III) develop field-deployable (on-site) applications using the established bioaffinity-based systems.

Accomplishments toward Project Goals

This final report includes the entirety of the timeline from January 2017 through December of 2020. This is included with the caveat that we were unable to complete any physical research after March of 2020 due to restrictions put in place during the COVID-19 pandemic. During this shutdown period, Dr. Jan Halamek and his lab relocated to Texas Tech University after resigning from the University at Albany, SUNY, as detailed in the previous letter regarding the funding extension. This ceased the funding of the project in August of 2020. Research has not been able to proceed since the March shutdown due to COVID-19-related research restrictions and consequent process of relocation of the laboratory and. We have been focusing on data correlation in lieu of physical data collection, since for several months we were not allowed to be in the laboratory and physically conduct further research. This final report will contain a summary of all accomplishments thus far.

Since the previous report, we have also begun to develop a portable system to noninvasively correlate sweat ethanol levels to blood alcohol concentrations. This developed system produces a visible color change, for which we have also developed a smartphone application capable of correlating the intensity of the color produced to blood alcohol concentrations. Although we have mostly focused on the collection of sweat for our initial proof-of-concept projects, we plan to continue to optimize our systems to work with the low levels of analyte expected to be found in fingerprints. The transition from sweat to fingerprints will further enhance the roadside capabilities of the developed systems.

Project Objectives

1. ***Objective 1****:* Mass spectrometric (MS) identification and quantification of individual or pools of amino acids, which constitute valid determinants of the personal attributes (ethnicity) and indirect personal characteristics (effect of food intake – vegetarian/omnivore) of the fingerprint originator.

Summary

We applied the previously developed and optimized GC-MS measurement system for lactate, urea, and L-alanine towards a large-scale biometric monitoring study. Three women volunteered to provide sweat via pilocarpine iontophoresis for 21 days over a 40-day time span. Each day, their metabolite levels were evaluated by both GC-MS analysis and the optimized bioaffinity-based assays previously detailed in Objective 2. Our accomplishments towards Objective 1 focus on the statistically evaluation and relevance of the data collected during the biometric monitoring study.

1.1.1. Experimental work

Gas chromatography-mass spectrometry (GC-MS) was utilized to carry out the initial analysis of fingerprint extracts. This work relied on a Hewlett Packard 6890 Series GC System coupled with a 5972 Mass Selective Detector (MSD) and supported by MassHunter software. The rather polar nature of amino acids implies that these analytes must be derivatized to enable the vaporization necessary for GC-MS analysis. Different derivatization strategies have been developed over the years, which increase not only the hydrophobicity/volatility of amino acids, but also their stability during analysis. We opted to utilize a silylation reaction that has been proven very effective in previous studies.[1] After trying several amino acids for biometric identification, it was decided that some were just not able to be optimized enough or weren't as readable using our method. This included L-aspartic acid and L-glutamic acid, which were found in any of the analyzed fingerprint samples, the GC-MS method and extraction are not sensitive enough to detect them. We further optimized the reaction conditions by using the finalized markers, L-alanine, glycine, and urea standards. Individual 10 mM samples of each analyte were separately treated with a 1:1 mixture of N-tert-butyldimethylsilyl-N-methyltrifluoroacetamide (MTBSTFA) and acetonitrile at 85°C for 30 min. By reacting with active nucleophilic groups on polar molecules, this derivatizing agent forms tert-butyl dimethylsilyl (TBDMS) derivatives that are rather hydrophobic. Additionally, an equimolar 10 mM mixture of the four standards was treated with MTBSTFA in identical fashion before GC-MS analysis. For each set of analyses, concurrent methanol samples and extraction blanks were analyzed to verify the absence of any amino acid traces.

Table 1. GC-MS Instrumental Parameters

Oven	100 °C (1 min.), 17 °C/min. to 117 °C (3 min.), 40 °C/min. to 300 °C, post run 250 °C (5 min.)
Injection Temperature	250 °C
MSD Interface	325 °C
Scan Range	m/z: 40-450
Carrier Gas	Helium, 1 mL/min., constant
Injection	1 µL, splitless

We subsequently applied the entire analytical workflow, which included extraction, derivatization, and GC-MS analysis, to evaluate the, metabolite content of authentic sweat samples, as outlined in recent publications. The extraction procedure provides a small quantity of sweat, which must be fully evaporated before derivatization. To this end, a method was developed to dry down the extracts, which involved incubation of each sample at 85°C for approximately 1.5 hr, or until fully dry. MTBSTFA reaction can then be performed directly on the evaporated material to enable GC-MS analysis. Three female volunteers provided sweat via pilocarpine

iontophoresis for 21 days for the bioaffinity-based analysis of lactate, urea, and L-alanine. Each analyte was test in triplicates on each day. The collection period spanned 40 days, which included 5-6 weeks of data collection.

1.1.2. Significant results

Previous work on this project has established that the derivatives of each metabolite (lactate, urea, and L-alanine) can be identified based on its characteristic mass-to-charge ratios as listed in Table 2. A spread of the data collected for lactate has been included in Figure 1 to show the slight daily differences in concentrations amongst the three individuals, while a general trend was maintained.

Table 2: Metabolite standard derivatives, GC retention times, and mass to charge ratios.

Compound	Derivative	Retention time (min)	Mass-to-charge (m/z)
L-alanine	L-alanine, 2 TBDMS	7.546	158, 73, 232, 260, 133
Lactate	lactate, 2 TBDMS	7.298	147, 73, 261, 189, 233
Urea	urea, 2 TBDMS	8.024	231, 147, 73, 132, 132

In order to determine if the analytical responses for each individual over time are unique to the sample originator and statistically different from other individuals in this study, both MANOVA and ANOVA tests were performed. This analysis was performed on the average daily responses for each metabolite using both the UV-Vis based method and the GC-MS based method. MANOVA is a method of statistical analysis capable of comparing means for multiple dependent variables across two or more groups.[2] A low p-value supports that there is a significant statistical difference between each individual when considering the three analytes (lactate, urea, and L-alanine) on each day of analysis simultaneously. ANOVA is capable of comparing means in order to evaluate the significance of each dependent variable (metabolite) separately.

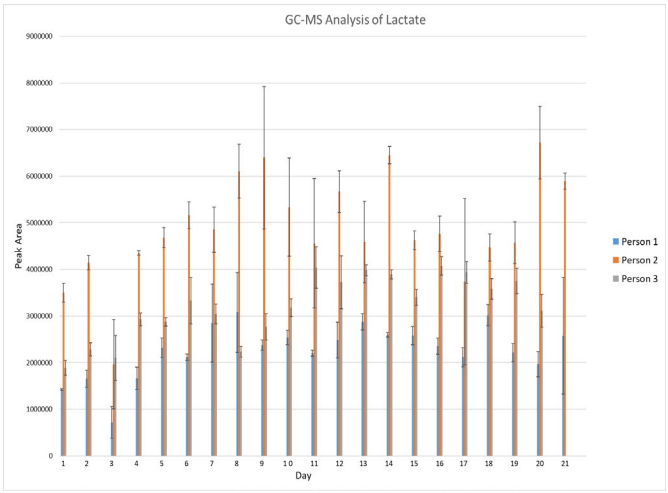

Figure 1: GC-MS analysis of 1 µL sweat for lactate detection in three individuals over 21 days.

Table 3 lists the statistical p values obtained from the MANOVA and ANOVA analyses.

Table 3. MANOVA and ANOVA results for GC-MS based metabolic analysis methods

	GC-MS
MANOVA	p < 1.31e-10 ***
ANOVA (Lactate)	p < *4.402e-14* ***
ANOVA (Urea)	p < *0.006675* **
ANOVA (Alanine)	p < *0.1281*

The p-values from the MANOVA tests for the GC-MS data sets were calculated to be < 0.001. A low p-value supports that there is a significant statistical difference between each individual when considering the responses from all three analytes (lactate, urea, and L-alanine) together. Due to the significance of the MANOVA tests, an analysis of variance (ANOVA) test was performed for each variable (metabolite) of the GC-MS samples. The purpose of the ANOVA test is to establish

the significance of the individual dependent variables. For, GC-MS based analysis, only one of the three ANOVA test, specific for lactate detection, calculated a p-valued < 0.001. These results support that a panel of markers can be used to statistically differentiate individuals using GC-MS analysis, however, a single marker alone may not be enough.

This work also seeks to determine if each individual's metabolite levels vary depending on the day of analysis. In order to evaluate the correlation between each metabolite and time, correlation circles of partial least squares regression was applied to the GC-MS sample set. Correlation circles of partial least squares (PLS) regression are commonly used in genomic and metabolomics studies in order to extract meaningful, biological data from complex data and can be used to visualize the relationship between multiple variables.[3] Variables in close proximity to each other are considered to be more strongly correlated than variables that are farther apart within the two dimensional circle.

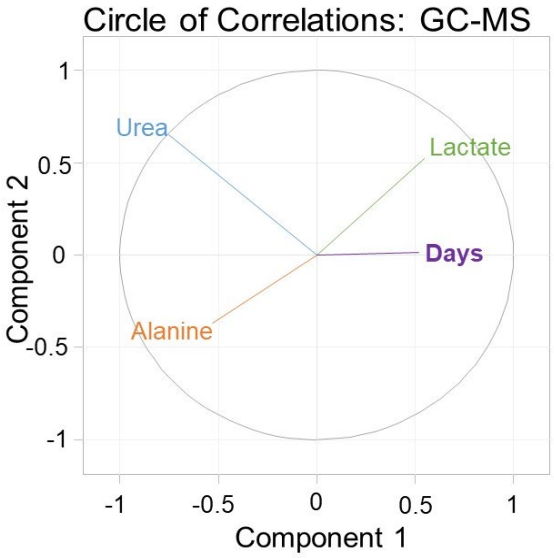

Figure 2. Correlation circle of PLS regression for the GC-MS based analysis.

The correlation circle of partial least squares (PLS) regression can be seen in Figure 2. This figure illustrates the correlation of the variables with the first two components associated to the first two latent variables. It is important to note that there is a significant distance between each metabolite and as well as the day of analysis. This means that the lactate, urea, and L-alanine concentrations are not correlated with each other or with the day of analysis.

1.1.3. Conclusions

This study will allow us to evaluate the potential of a metabolite panel to distinguish individuals. The p-values from the MANOVA tests for the GC-MS data sets were calculated to be < 0.001, A low p-value supports that there is a significant statistical difference between each individual when considering the responses from all three analytes (lactate, urea, and L-alanine) together. For, GC-MS based analysis, only one of the three ANOVA test, specific for lactate detection, calculated a p-valued < 0.001. **These results support that a panel of markers can be used to statistically differentiate individuals using GC-MS analysis, however, a single marker alone may not be enough.** This will be essential to validate the specific correlations used to design our bioaffinity assays.

***2. Objective 2**:* Design and optimization of the bioaffinity-based assay protocols for the determination of originator characteristics based on the MS-identified targets, followed by evaluation of relevant cascade systems using authentic fingerprint samples.

Summary

Several different experiments have been conducted to work towards this objective:

a. Feasibility of determining biological sex using only one biomarker (alanine/arginine)

In order to determine if decreasing the number of amino acid targets is a viable option, we decided it was important to take our previously established concept of biological sex identification and combine it with a bioaffinity-based assay for the detection of only alanine and one for only arginine. The results displayed here are the first of their kind, in that the two single amino acid assays – a bioaffinity-based assay for alanine and a chemical assay for arginine – are fully capable of distinguishing between sexes using just the contents of fingerprints.

b. *Lactate, urea, and glutamate quantification for biometric purposes*
The expected concentration ranges of lactate, urea, and glutamate are significantly different in sweat samples between individuals. This is important because the variation of an individual's level of each metabolite is proportional to the concentration. For example, the concentration of lactate is the most abundant and the most variable, whereas the concentration of glutamate is the least abundant and least variable of the three metabolites. The combined results of the three metabolite analyses has the ability to provide substantial information about the sample originator, such as his/her unique lactate, urea, and glutamate concentrations.

c. *Optimizing our currently developed fingerprint extraction method*
For this objective, a large portion of the experimental process was focused on determining if the fingerprint extraction protocol was using optimal conditions. The results shown here will demonstrate the effect of modifying the extraction protocol. If the original protocol conditions were not ideal, there is a chance that it is missing certain amino acids or that it is encompassing a group of amino acids that has a lower affinity for the assay being used. The modifications that were utilized included changing the acid used, adjusting the pH of the acid solutions, as well as adding a detergent.

d. *Evaluating how time since deposition (TSD) can affect our fingerprint samples*
Given that fingerprints are composed of biological compounds that naturally decompose over time, the next logical step for our group was to continue to target these compounds with respect to their decomposition. Our main goal was to determine how long the differentiation between an aged female fingerprint and fresh male fingerprint could be made using the system developed by our laboratory. This work will demonstrate that our system is not limited to use with "fresh" fingerprint samples.

e. *Ketone Body monitoring in sweat*
We began testing ways to analyze ketone bodies in sweat. This system has value for diabetic patients and medical professionals. For diabetics, it is important to track the concentration of circulating ketone bodies in order to prevent ketoacidosis. An accumulation of ketone bodies in the body can lead to ketoacidosis, and ultimately, metabolic acidosis.[4] For diabetic patients, an excess of ketone bodies in the blood can be life threatening. β-HB makes up approximately 75% of the ketone bodies found in serum and are often measured in blood to diagnosis ketoacidosis.[5-7] These blood tests are invasive and require medical professionals for testing and analysis processes. This spin-off concept aims to develop an earlier diagnosis process that can be implemented as a portable test that is non-invasive, fast, accurate, and user friendly. The concentration of ketone bodies in the body fluctuates based on factors such as differences in basal metabolic rates and hepatic glycogen stores.[8] Therefore, it is necessary to distinguish

between healthy and pathologic concentration ranges. In general, healthy ketone body ranges have been determined to be less than 0.5 mM, whereas concentrations over 1 mM are classified as hyperketonemia, and any levels over 3 mM are evident of diabetic ketoacidosis.[8] These values were used as a range to optimize this biochemical detection system.

f. Completion of a biometric monitoring study using sweat samples and selected biomarkers
We evaluated sweat content, specifically lactate, urea, and L-alanine, from three individuals over an extended period of time. For this study, we used the newly developed sweat collection process and three different enzymatic assays to detect each metabolite. Secondly, we applied this monitoring data to our encryption abilities, with a goal of demonstrating that human sweat can be used to secure private information.

This work ultimately aims to demonstrate the collective ability of compounds inherent in sweat to differentiate individuals based on his/her person-specific metabolic patterns.

2.1.1 Experimental work

a. Feasibility of determining biological sex using only one biomarker (alanine/arginine)

Fingerprint samples were collected from two groups of volunteers, 25 Caucasian males and 25 Caucasian females on polyethylene film. Following the extraction, the fingerprint samples containing the amino acid were subjected to the single analyte bioaffinity-based assay specific for alanine. This assay utilized the enzymes alanine transaminase (ALT, 2.6.1.2), pyruvate oxidase (POx, E.C. 1.2.3.3), and horseradish peroxidase (HRP, E.C. 1.11.1.7). The assay uses alanine as the substrate for ALT, which drives the conversion of a corresponding amount of KTG into pyruvate. The pyruvate (Pyr) is then used as a substrate for POx in order to produce H2O2, which is subsequently consumed by HRP to cause the oxidation of 2,2'-azino-bis(3-ethylbenzothiazoline-6-sulphonic acid) (ABTS) to produce an optical signal, measurable at 405 nm.

For arginine detection, a known method called the Sakaguchi test was used, the guanidine group within the structure of arginine reacts with α-naphthol and hypobromite under alkaline conditions (10% sodium hydroxide). This results in the production of a red-colored complex which can be measured at 500 nm. The manuscript containing both methods was accepted in Analytical Chemistry in December 2017.

These analyses were conducted on both mimicked and authentic fingerprints.

b. Lactate, urea, and glutamate quantification for biometric purposes

Sweat samples were collected from two groups of volunteers, 13 Caucasian males and 12 Caucasian females according to an established procedure successfully applied in our most recent publication.2 This process involves the use of a 7.5 cm x 1 cm section of a Johnson and Johnson BAND-AID brand medium non-stick pad. This sweat-collection pad was placed on the forearm of each volunteer and held in place with athletic tape. To aid in sweat production, a 1 inch black silicone wristband was placed on top of the taped sweat pad. Participants exercised for 30 minutes to guarantee sufficient sweat production to fully saturate the sweat pad. An extraction method was then used to remove the sweat from the pad, which mirrors the fingerprint extraction previously developed by the Halamek Lab. Each sweat pad was cut into 9 identical pieces for triplicate analysis by each enzymatic assay. Next, each sample was incubated in 120 µL of 10 mM HCl for 20 minutes at 40 °C. Finally, centrifugation was utilized

to obtain 100 µL of sweat for analysis. Following the extraction, the sweat samples containing the desired metabolites were separately subjected to three, single-analyte bioaffinity-based assays specific for lactate, urea, and glutamate.
The spectrophotometer UV/Vis temperature-controlled plate reader (SpectraMax Plus 384, Molecular Devices, CA), was used to take optical measurements of the samples 37 °C via kinetic mode at λ = 405 nm. A microtiter polystyrene (PS, Thermo Scientific) plate was utilized.

Method for Detection of Lactate

The assay for lactate determination consists of lactate oxidase (LOx, E.C. 1.13.12.4) and horseradish peroxidase (HRP, E.C. 1.11.1.7). LOx is an enzyme specific for consumption of lactate and oxygen (O2) to produce pyruvate and hydrogen peroxide (H2O2). HRP uses H2O2 as a substrate in order to oxidize the ABTS dye (2,2'-azino-bis(3-ethylbenzothiazoline- 6-sulphonic acid)) and generate a visible increase in absorbance at 405 nm. This system is realized in potassium phosphate buffer pH 7.6 containing 0.1 U LOx, 0.2 U HRP, and 1 mM ABTS.

Method for Detection Urea.

The assay for urea detection utilizes both urease (UR, E.C. 3.5.1.5) and glutamic dehydrogenase (GlDH, E.C. 1.4.1.3). UR is an enzyme specific for hydrolysis of urea to produce ammonium. GlDH consumes the ammonium, KTG, and NADH as substrates to produce glutamate and NAD+. This conversion of NADH to NAD+ generates a decrease in absorbance at 340 nm. This two-enzyme cascade was optimized and realized in 1 M Tris-HCl buffer pH 7.8 containing 1 U UR, 1 U GlDH, 0.5 mM KTG, and 0.3 mM NADH.

Method for Detection of Glutamate.

The assay for glutamate detection utilizes GlDH which consumes glutamate and NAD+ as substrates. This reaction results in the production of KTG, ammonium, and NADH. The conversion of NAD+ to NADH generates a visible increase in signal at 340 nm. This single enzyme assay was optimized and realized in 0.2 M TEA buffer pH 7.6 containing 1 U GlDH and 1 mM NAD+.

c. Optimizing our currently developed fingerprint extraction method

Extraction Protocols

The original fingerprint extraction first published in 2016[9] is conducted using real fingerprints as opposed to amino acid standards. To obtain the fingerprints, a person's thumb is rubbed against their forehead and then pressed against a piece of polyethylene film (generic plastic wrap).[10] A 1 cm x 2 cm rectangle is cut away from the fingerprint and placed in a 1.5 mL microcentrifuge tube. To this cutout, 120 µL of 10 mM HCl is added. The sample is then vortexed for two minutes followed by an incubation period at 40 ºC for 20 minutes. After this incubation period, the plastic wrap is removed from the solution and 100 µL of the sample is then used for analysis in each chemical assay.

In the work described here, the process of extraction is similar to the original protocol, however, several modification steps were used in order to improve the efficacy of extracting the amino acids from the fingerprints. There were two approaches that were used to modify

the original extraction protocol in order to find the most effective way to extract the amino acids from the fingerprints. One modification that was chosen was to vary the pH of the HCl that was used. Originally, 10 mM HCl with a pH 2.15 was used. In order to see the effect of changing the pH, HCl pH 1.06, pH 2.08, pH 3.22, pH 4.12 and pH 5.04 were used.

The second modification, where acetic acid was used instead of HCl, involved acetic acid at pH 2.04, pH 3.03, and pH 4.05. There are only three variations in the pH values for acetic acid due to the fact that the resting pH of pure acetic acid is greater than pH 1.0 and that even one drop of acetic acid lowered the pH of ultra-pure water below pH 5.0. The change in pH for the extraction as well as the change in the particular acid used was assessed using both the ninhydrin assay and the Bradford assay.

The final modification to the extraction protocol included introducing 0.25% (v/v) Tween 20 to the fingerprint solution prior to vortexing and the incubation period with the intentions of extracting more amino acid content. This modification was employed along with the best acid and pH pairing from the previous modification experiments and both the ninhydrin assay and the Bradford assay were used for assessment of the extraction modifications.

The Ninhydrin Chemical Assay

Ninhydrin reacts with L-amino acids present in the fingerprint extract in order to generate aldehydes, ammonia, and carbon dioxide. Through this process, ninhydrin is also partially reduced. Remaining ninhydrin then condenses in the presence of the ammonia and the partially reduced ninhydrin to produce diketohydrindylidene-diketohydrindaminean (DYDA) which is the cause of the intense blue-purple color known as Ruhemann's purple. Ultimately, this production of color can be measured via Ultraviolet-Visible spectroscopy (UV-Vis) – specifically, a Molecular Devices Spectramax 384 spectrophotometer was used for all studies. The scheme for this reaction can be seen in Scheme 1.

To simplify the chemical assay for future use by law enforcement, a premade solution of ninhydrin was purchased from Sigma Aldrich. This solution consisted of 2% ninhydrin and hydrindantin in DMSO along with lithium acetate buffer pH 5.2. This would be used for all future work in replacement of the 52.53% (v/v) ninhydrin dissolved in DMSO, 10.53% glycerol, and 0.1 M citrate buffer pH 5.5 which were used in the original publication.[9] To test the efficacy of the premade solution in comparison to the previously published methods, the ratios of the premade solution versus water and citrate buffer were varied. A glycine standard – 33 μM in the microtiter plate – was used for the purpose of having an optimal response before working with significantly lower amino acid concentrations that are found in a fingerprint sample. After several variations were tried, the final ratio of reagents was 1:1:1 (equal volumes of 100 μL) of ninhydrin solution, fingerprint sample, and citrate buffer. In both methods, the maximum wavelength (λ_{max}) for the expected color was 570 nm.[11-13]

The Bradford Chemical Assay

The second chemical assay that was used for these experiments was the Bradford assay, published in 2017 for use with fingerprint analysis.[14] In this reaction, the Bradford reagent – comprised of Coomassie Brilliant Blue G-250 dye, methanol, and phosphoric acid – reacts with six amino acids (arginine, histidine, lysine, phenylalanine, tyrosine, and tryptophan) that are present in the fingerprint extracts. For this assay, 150 μL of the commercially available Bradford Reagent is combined with 50 μL of water and 100 μL of the extracted fingerprint

sample. The scheme for this reaction is shown in Scheme 2. For the Bradford assay, the λ_{max} of the colored product was 595 nm.[15-18]

d. Evaluating how time since deposition (TSD) can affect our fingerprint samples

To begin this pilot study into the age of a fingerprint, 70 fingerprints – 5 fingerprints for 14 different time points – were collected on PEF for each chemical assay and left to age on a lab bench at room temperature. These samples were collected from a single female volunteer in order to limit possible variations in responses. It is acknowledged that there is some variation from person to person as seen in previous publications,[1,9,14] and this effect in conjunction with fingerprint TSD will be assessed in the future. Likewise, the PEF was the only surface used for these analyses to limit the variation expected from different surfaces during this preliminary investigation into TSD using these chemical assays.

The time frame of fingerprint TSD included fresh fingerprints ("Day 0"), along with a set of 5 "aged" fingerprints each day for 7 days, followed by a set of 5 "aged" fingerprints once a week at days 14, 21, and 28. The study concluded with analyses of 5 "aged" fingerprints after 42 days, 63 days, and 84 days. Additionally, a set of five fresh male fingerprints were collected on PEF and were extracted for immediate analysis. As previously mentioned, the chemical assays utilized were modified versions of the 2016 ninhydrin[9] and 2018[1] Sakaguchi chemical assays as well as the original 2017[14] Bradford assay.

Furthermore, with respect to limiting variation in responses, the intention was to keep a stable room temperature throughout the duration of the aging experiment. Ideally this would have been 70 ºF, as indicated by the laboratory thermostat.

e. Ketone Body monitoring in sweat

For the analysis of ketone bodies in person's sweat, a single-analyte enzymatic assay was used for the detection of β-hydroxybutyrate (β-HB). This system requires two sets of reactions, the first leads to the production of NADH, which is invisible to the naked eye. As a result, a second reaction is needed for visualization purposes. In this step, the production of a formazan dye is visible at 580 nm. This assay is depicted in Scheme 1.

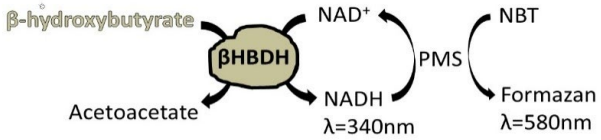

Scheme 1. The biocatalytic cascade for determination of β-hydroxybutyrate content in buffered samples.

Method for Detection of β-Hydroxybutyrate

The assay for β-HB determination, depicted in Scheme 1, utilizes 3-hydroxybutyrate dehydrogenase (βHBDH; E.C.1.1.1.30).[19] This enzyme converts β-HB into acetoacetate in the presence of the oxidizing reagent, NAD^+. This results in the reduction of NAD^+ to NADH, which generates an increase in absorbance at 340 nm – which is invisible to the naked eye. This system utilizes 100 mM Tris-HCl buffer pH 7.8 containing 50 mU βHBDH, and 500 µM NAD^+.

Method for Visualization of β-Hydroxybutyrate

After this initial reaction is completed, β-HB is visualized by the addition of PMS and NBT. PMS is added in order to mediate the second reaction, where NADH reduces NBT to a colored product, a formazan dye, which can be measured spectrophotometrically at 580 nm. For this step, 6 μM PMS and 100 μM NBT were used. Here, the amount of formazan dye produced is directly proportional to the amount of β-HB in the sample.

Method for Image Quantification of β-Hydroxybutyrate

Following the completion of the second reaction, a standard of 4 μM Nile Blue A dye was added to the adjacent wells for each sample. Images were taken of each well with the neighboring Nile Blue A standard. These images were acquired using the MiScope-MP2 and Video ToolBox software. Next, Fiji (formerly Image J) software was used to calculate the mean gray value of each sample and Nile Blue A standard well. The mean gray value is defined as the average gray value of a selected area, or the sum of the pixel gray values in the selected area divided by the number of pixels.[20] Using the red, green, blue (RGB) values from the images in this study, this value can be calculated by converting each pixel to grayscale via the following formulas:

Option 1: $gray = \frac{(red\ value + green\ value + blue\ value)}{3}$.

Option 2: $gray = (0.299 * red\ value) + (0.587 * green\ value) + (0.114 * blue\ value)$

The average and standard deviation of the mean gray values were calculated for each sample (n=3). The average sample response was divided by the equivalent average of Nile Blue A standards in order to create a mean gray value versus a standard.

f. Completion of a biometric monitoring study using sweat samples and selected biomarkers

Biometric Monitoring Study

The bioaffinity-based assays for the detections of lactate, urea and L-alanine from sweat were chosen for the biometric monitoring study with comparative analysis via GC-MS. These systems were previously optimized and are depicted in Schemes 1, 2, and 3. It was determined that 1 μL of sweat was required for analysis of lactate, 2 μL of sweat was required for analysis of urea, and 3 μL of sweat was required for analysis of L-alanine. These values allowed for comparisons between both modes of detection (GC-MS and bioaffinity based assays). Three female volunteers provided sweat via pilocarpine iontophoresis for 21 days for the bioaffinity-based analysis of lactate, urea, and L-alanine. Each analyte was test in quintuplets on each day. Three female volunteers provided sweat via pilocarpine iontophoresis for 21 days for the bioaffinity-based analysis of lactate, urea, and L-alanine. Each analyte was tested in triplicates on each day.

Lactate Detection via Bioaffinity-based Assay

The assay for lactate determination, depicted in Scheme 2, consists of lactate oxidase (LOx, E.C. 1.13.12.4) and horseradish peroxidase (HRP, E.C. 1.11.1.7). LOx is an enzyme specific for consumption of lactate and oxygen (O_2) to produce pyruvate and hydrogen peroxide (H_2O_2). HRP uses H_2O_2 as a substrate in order to oxidize the ABTS dye (2,2'-azino-bis(3-ethylbenzothiazoline-6-sulphonic acid)) and generate a visible increase in absorbance at 405 nm. This system is realized in potassium phosphate buffer pH 7.6 containing 0.1 U LOx, 0.2 U HRP, and 1 mM ABTS.

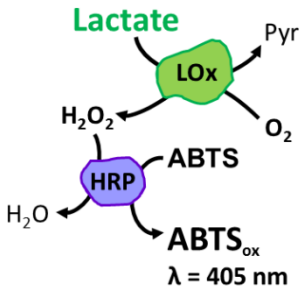

Scheme 2. The biocatalytic cascade for determination of lactate content in both mimicked and authentic sweat samples.

Urea Detection via Bioaffinity-based Assay

The assay for urea detection, depicted in Scheme 3, utilizes both urease (UR, E.C. 3.5.1.5) and glutamic dehydrogenase (GlDH, E.C. 1.4.1.3). UR is an enzyme specific for hydrolysis of urea to produce ammonium. GlDH consumes the ammonium, KTG, and NADH as substrates to produce glutamate and NAD^+. This conversion of NADH to NAD^+ generates a decrease in absorbance at 340 nm. This two enzyme cascade was optimized and realized in 1 M Tris-HCl buffer pH 7.8 containing 1 U UR, 1 U GlDH, 0.5 mM KTG, and 0.3 mM NADH.

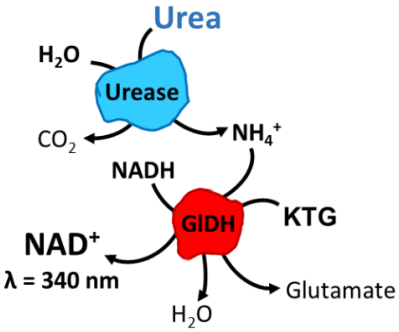

Scheme 3. The biocatalytic cascade for determination of urea content in both mimicked and authentic sweat samples.

L-alanine Detection via Bioaffinity-based Assay

The assay for L-alanine detection, depicted in Scheme 4, is a double enzyme system. The first enzyme, alanine aminotransferase (ALT), consumes L-alanine and KTG as substrates. Next, lactic acid dehydrogenase (LDH) converts the produced pyruvate to lactate while simultaneously oxidizing NADH to NAD+. The conversion of NADH to NAD+ generates a visible decrease in signal at 340 nm. This single enzyme assay was optimized and realized in 1.0 M Tris-HCl buffer using 0.5 U ALT, 0.5 U LDH, 1 mM KTG, and 0.25 mM NADH.

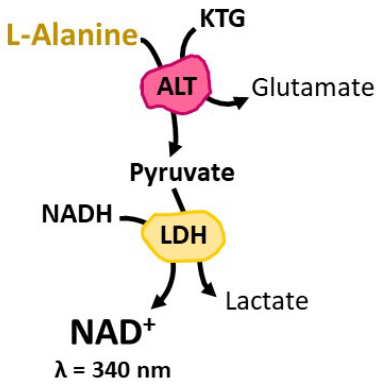

Scheme 4. The biocatalytic cascade for determination of L-alanine content in both mimicked and authentic sweat samples.

Encryption Application Concept

The biometric responses collected from the monitoring study were further applied towards encryption.

2.1.2. Significant results

a. *Feasibility of determining biological sex using only one biomarker (alanine/arginine)*

ALT/POx/HRP Assay: These results were analyzed ROC analysis. The Area Under the Curve (AUC) for the mimicked samples, was 0.82 which means that there was an 82% chance of correctly classifying the results. This is relatively low for what we would like, however it is most likely because the concentrations of predetermined and randomly grouped together which leaves room for extensive overlap. For the authentic samples, the AUC was 0.998 or 99.8% probability. These are depicted in Figure 3. This was much more acceptable for what we look for and more consistent with our expectations.

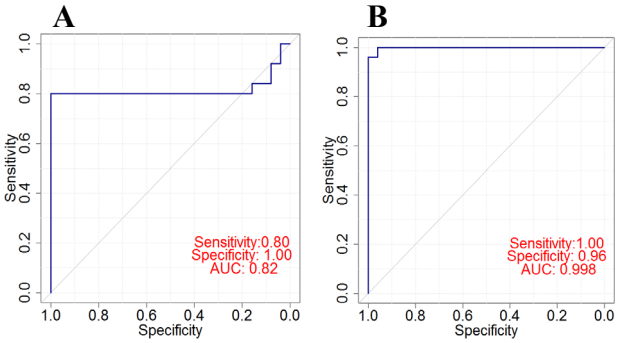

Figure 3. The results of ROC/AUC analysis of the (A) mimicked samples and (B) authentic fingerprint samples analyzed by the ALT/POx/HRP assay.

Sakaguchi Assay: The AUC for the mimicked samples was 1.0 which means that there was a 100% chance of correctly classifying the results. For the authentic samples the AUC was also 1.0 or 100% probability, as seen in Figure 4.

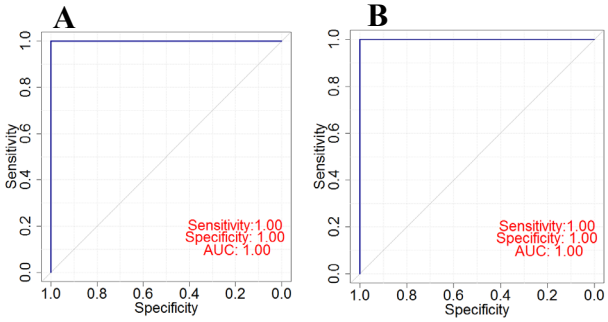

Figure 4. The results of ROC/AUC analysis of the (A) mimicked samples and (B) authentic fingerprint samples analyzed by the Sakaguchi test.

b. *Lactate, urea, and glutamate quantification for biometric purposes*

The combination of all three ΔAbs values at 12 minutes for urea and glutamate detection and 2.5 minutes for lactate determination were used to create the 3D scatter plot in Figure 5. A different time point was chosen for authentic lactate samples due to the high lactate concentrations in authentic samples that caused the reaction to completed well before 12 minutes of analysis. This 3D plot demonstrates that no two authentic sweat samples overlap when considering all three analytes. Additionally, the p-value from the MANOVA test for the authentic samples was calculated to be < 0.001. A low p-value supports that there is a significant statistical difference between each individual when considering the responses from all three analytes (lactate, urea, and glutamate) together. Due to the significance of the MANOVA test, an analysis of variance (ANOVA) test was performed for each variable (metabolite). The purpose of the ANOVA test is to establish the significance of the individual dependent variables. Each of the ANOVA tests calculated p-values < 0.001. The low p-values demonstrate that there is a significant statistical difference between each individual when considering only one analyte. Overall, these statistical analyses support the ability of the set of markers together, as well as each marker separately, to distinguish individuals.

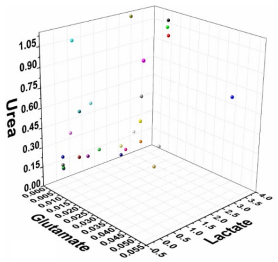

Figure 5. 3D scatter plot with the average (N=3) ΔAbs. value for lactate, urea, and glutamate from 25 authentic sweat samples. The x-axis corresponds to glutamate, the y-axis corresponds to lactate, and the z-axis corresponds to urea at 12 minutes, 2.5 minutes, and 12 minutes of reaction time, respectively. Each sphere in the plot represents one individual person using the aforementioned x, y, and z values.

c. *Optimizing our currently developed fingerprint extraction method*

pH Studies: For all pHs that were used with the Sakaguchi assay, the λ_{max} remained consistent with the expected value. Most notably within these results was the significant increase in absorbance when pH 1.06 was used. There was also an increase in absorbance for pH 4.12 and 5.04, but they were still lower than the pH 1.06 response. Based on these results, it was determined that when using the ninhydrin assay, a pH 1.06 provided a more efficient amino acid extraction than the initial 10 mM (pH 2.15) HCl solution because it generated an improved absorbance with plenty of room for the absorbance at λ_{max} to decrease when conducting further research into aging of fingerprints and for future work that may utilize significantly lower amino acid concentrations. With acetic acid used instead, the pH 2.04 and pH 3.03 did not generate a response that was comparable to the original method; only the response for the acetic acid pH 4.05 showed approximately the same response as the original method. However, the response from the HCl pH 1.06 was still superior, indicating that HCl was the optimal choice of acid for extraction and the pH 1.06 was the optimal choice of pH. For the Bradford trials, there was a drastic peak shift to approximately 650 nm – with a λ_{max} in a similar location to the blanks but at a higher absorbance. This result was somewhat expected given the Bradford reagent is pH sensitive. Given that the λ_{max} was out of the range of accepted values for all HCl solutions except for the original solution, it was determined that the original method was, in fact, the optimal extraction protocol. When switching to acetic acid again, pH 2.04 had an absorbance response at about the same intensity as original protocol. However, just as was seen with the HCl pH variations, the λ_{max} for all three acetic acid pHs shifted to a wavelength of 650 nm which, again, is outside of the accepted range.

Tween detergent studies: The addition of 0.25% (v/v) was implemented with the best acid and pH from the previous set of studies for each assay. More specifically, Tween 20 was added to the HCl pH 1.06 solution when using the ninhydrin assay and to the 10 mM (pH 2.15) HCl solution when using the Bradford assay.. For the ninhydrin assay, both the original 10 mM (pH 2.15) HCl and the pH 1.06 HCl solutions were tested with and without the addition of Tween 20. While the λ_{max} remained at 570 nm, the presence of Tween 20 significantly decreased the absorbance for both HCl solutions. Furthermore, the pH 1.06 HCl continued to have a higher response than the original solution which again confirmed the analysis from the first extraction modification experiments. For the Bradford assay, only the original 10 mM (pH 2.15) HCl solution was tested with and without the presence of Tween 20. The presence of Tween 20 did increase the absorbance rather significantly as compared to the response of the Bradford assay without Tween 20. However, the λ_{max} shifted to just on the edge of the acceptable range at approximately 615-620 nm. The other problem is that it is known that detergents can have a negative effect of assays such as the Bradford assay. While detergents have a lesser effect on the Bradford assay as compared to other biochemical methods, there is still a certain threshold that needs to be maintained with regard to the amount of Tween 20 versus the amount of Bradford reagent present. As such, there is no clear indication as to whether the increase in absorbance due to too much Tween 20 or is it is truly assisting in the amino acid extraction, despite the slight shift in λ_{max}. Based on the results shown here, it was determined that Tween 20 was not a beneficial component to improving the efficacy of the extraction protocol, regardless of the assay chosen for analysis.

d. *Evaluating how time since deposition (TSD) can affect our fingerprint samples*
Fingerprint TSD – Trial 1

The first TSD analysis was designed for 84 days (12 weeks) of experiments using the ninhydrin and Bradford assays, 70 fingerprints each. The Sakaguchi assay was not used in this initial study as the new protocol was still being optimized as the result of manufacturing setbacks. Additionally, the TSD concept was first tested using these methods because they are both multi-analyte assays which would afford the best absorbance responses. If fingerprint TSD could not be determined using systems whose responses are based on the sum of the targeted analytes, it would be unlikely that it would also not work with just a single analyte (arginine). The fingerprints were collected on a sheet of PEF and left fully exposed on a laboratory bench at room temperature. This environment provided the most authentic conditions to those expected at a crime scene since they were exposed to everyday particles from people walking by as well as light and temperature conditions that were not predetermined. "Day 0" indicates the samples that were collected and analyzed immediately to provide the control responses. As seen with both sets of results, there is a clear decreasing trend indicating that fingerprint TSD can be determined. Data for days 63 and 84 were not collected as there was no response generated from either assay. However, both assays were able to make the distinction between a female fingerprint and a male fingerprint for up to approximately 42 days (6 weeks), with more variation seen in the ninhydrin data.

There was one major obstacle that was encountered during this experimental process that contributed significantly to the variations seen in the results from both assays and to the rapid decrease in response seen in the ninhydrin assay results. When these experiments were established, the weather outside had become unseasonably cold, causing the temperature in the laboratory to decline. As a result, adjustments to the laboratory thermostat varied between 70 ˚F and 75 ˚F during this time period. Since the laboratory bench where the fingerprints were aging is located adjacent to the heater, it is believed that this had a major impact on the aging samples, as one would expect based on an increase in temperature and the knowledge of biological compound decomposition. It is also possible that with the

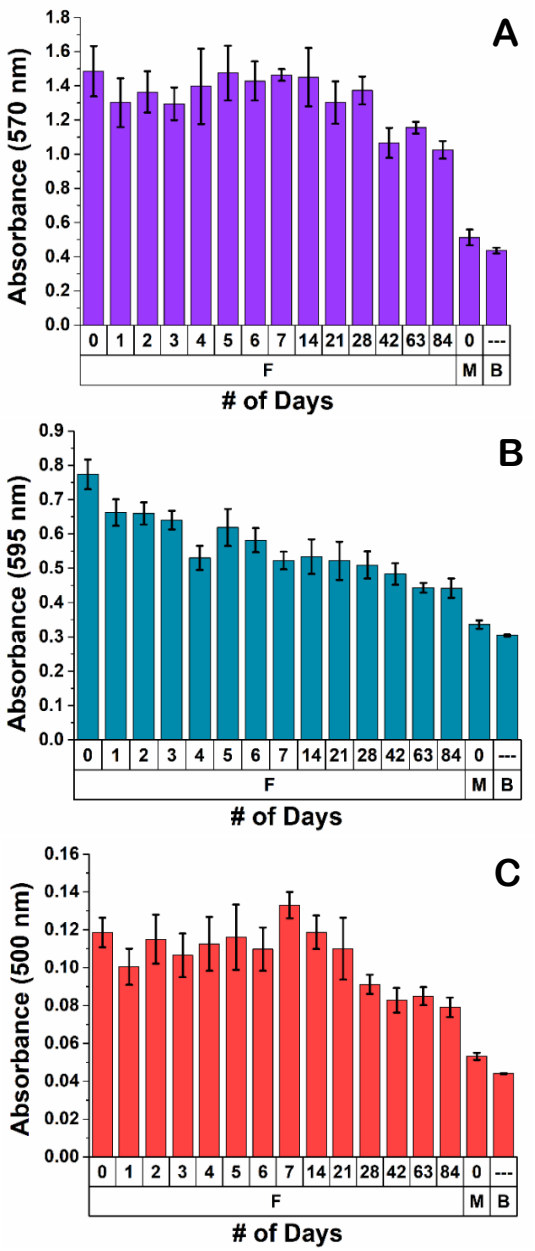

Figure 6. Second attempt at aging of fingerprints (n=5) analyzed by the chemical assays (A) ninhydrin assay; λ_{max} = 570 nm, (B) Bradford assay; λ_{max} = 595 nm, and (C) Sakaguchi assay; λ_{max} = 500 nm. The abbreviations shown are as follows: F = female, M = male, and B = blank.

heaters turned on, there was an increase in the amount of dust particles in the air, contributing to the fluctuations seen in the responses. Based on these deductions, the laboratory thermostat was monitored and held constant at 70 ˚F. As a result, the responses stabilized and began to gradually decrease. Despite this being an unintentionally uncontrolled environment, it does provide useful knowledge that crime scene conditions – specifically temperature – play a vital role in the ability to determine the TSD of a fingerprint as well as making the differentiation between a male and female fingerprint. This aside, it was determined that a difference could be established between a fresh male and an aged female fingerprint up to 42 days (6 weeks), even in an uncontrolled environment. However, this experiment was conducted a second time in order to establish a controlled TSD. For this experiment the thermostat was set at a constant 70 ºF and instructions were provided to not adjust the temperature. Additionally, since TSD was relatively successful with the ninhydrin and Bradford assays, it was determined that third set of 70 fingerprints would be added for analysis via the Sakaguchi assay.

Fingerprint TSD – Trial 2

In the second fingerprint TSD experiment, all three chemical assays were used to analyze 70 fingerprints collected on PEF for each assay across the same 14 time points as the previous experiment for 84 days (12 weeks) of fingerprint aging. This can be seen in Figure 6 above. There is a well-defined, decreasing trend. Remarkably, all three chemical assays were determined to be capable of differentiating between an aged female fingerprint and a fresh male fingerprint for up to 84 days. At the end of this study, the aged female samples were beginning to provide responses close to that of a fresh male sample but could still possibly make this differentiation with time points past the 84 days.

e. *Ketone Body monitoring in sweat*

Below are the results from the initial studies for the detection and quantification of βHB. These results for the detection via βHBDH (step 1), visualization via PMB/NBT, and image quantification using a camera and Fiji imaging software. All conditions were analyzed in a buffered solution using a range of expected physiological concentrations for β-HB from 0 to 1.0 mM. Figure 7A depicts increase in absorbance at 340 nm over time as a result of the enzymatic assay reducing NAD^+ to NADH. The Figure 7B displays the calibration curve from the data generated by the kinetic change in absorbance (ΔAbs.) responses (Fig. A) after 2 minutes of reaction time.

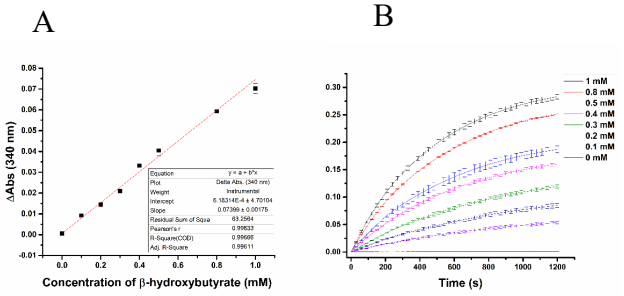

Figure 7. The detection of βHB in a buffer-based system spiked with physiological levels of analyte. (A) Kinetic change in absorbance response of the enzymatic reaction. (B) Calibration curve for the detection of β-HB at 2 minutes.

Next, Figure 8 depicts the second step of the reaction – the reduction of NBT via NADH – which produces a visible color (formazan dye). As before, Figure 10A displays the kinetic response of the assay following the introduction of PMS/NBT. Figure 10B takes this kinetic ΔAbs. data after 5.5 minutes of reaction time. Again, the amount of formazan dye produced is directly proportional to the concentration of β-HB in the sample. The final step is to numerically assess the color produced in step 2 (Fig. 10A) by collecting images of the visual color. As previously mentioned, images were taken of each reaction well along with its neighboring well containing the Nile Blue A standard. This dye served as a standard for comparison to limit the variation between images. Figure 9A and 9B show the visual color seen within these wells. These images were taken using the camera on an android smartphone as well as using the camera on the MiScope-MP2, respectively. In both images, the top row of wells contains the Nile Blue A dye standard and the bottom rows contain the decreasing β-HB concentrations as you move left to right. Next, Fiji (formerly Image J) software was used to calculate the mean gray value of each sample and Nile Blue A standard well. The formulas indicated above were used for this calculation. Once the mean gray value for each sample was calculated, it was plotted versus the sample's concertation in order to generate the respective calibration curve. Figure 9C displays the calibration curve for the Nile Blue A dye standard alone. With a correlation coefficient of 0.996, this standard demonstrates a direct, linear relationship between concentration and average mean gray value. Lastly, figure 9D displays the calibration curve correlating the concentration of β-HB to the mean gray value when the photo was taken with the camera on an android smartphone, while Figure 9E shows the calibration curve correlating the concentration of β-HB to the mean gray value when the photo was taken with the camera on the MiScope-M2. In both of these cases, the correlation coefficient was 0.909 – regardless of the camera that was used.

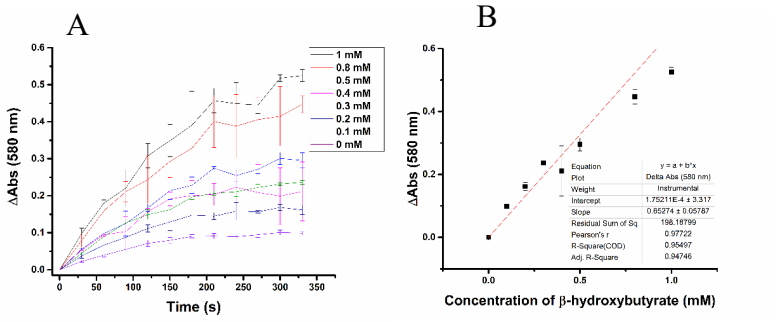

Figure 8. The visualization of β-HB in a buffer-based system spiked with physiological levels of analyte. (A) Kinetic change in absorbance response of the PMS/NBT chemical reaction. (B) Calibration curve for the detection of formazan dye at 5.5 minutes.

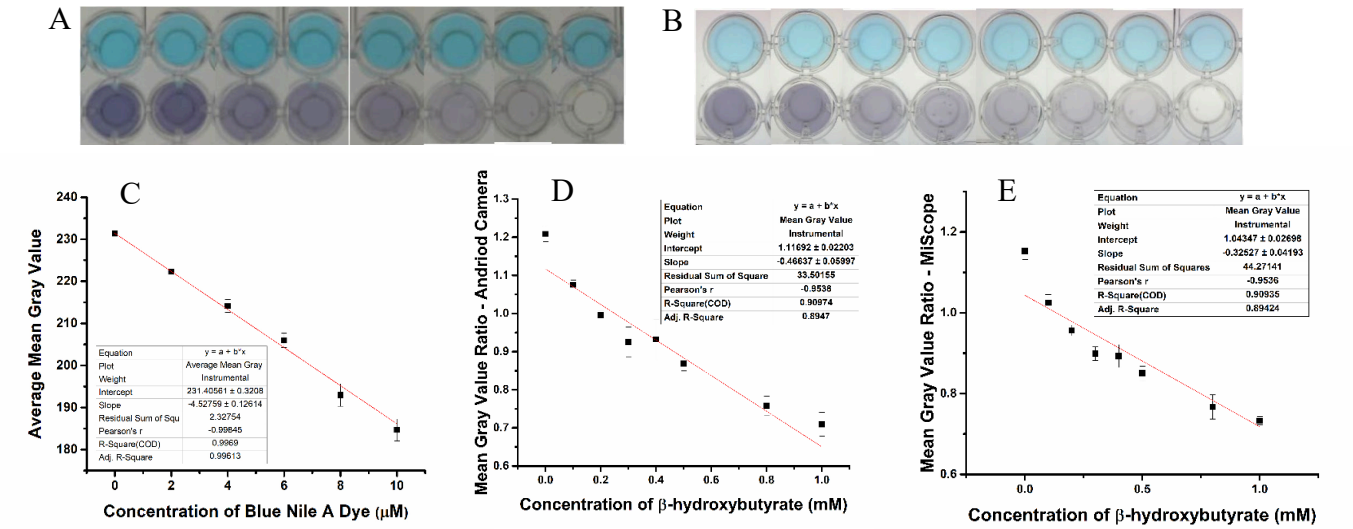

Figure 9. The image quantification of βHB in a buffer-based system spiked with physiological levels of analyte. The first two images are compilations of each β-HB concertation (n=1, assays were run in n=3 however) in the 96-well plate used for analysis. In both images (A & B), the top row of wells contains the Nile Blue A dye standard and the bottom rows contain the decreasing β-HB concentrations as you move left to right. (A) Image of the 96-well plate taken with an android cellphone and (B) Image of the 96-well plate taken with the camera on the MiScope-M2.

The final three images are the calibration curves generated from the mean gray values calculated from the images shown in the first two photos. (C) Calibration curve of Nile Blue A dye standard using the developed image quantification system. (D) Calibration curve correlating the concentration of β-HB to mean gray value using images taken with an android smartphone. (E) Calibration curve correlating the concentration of βHB to the mean gray value using images taken with the camera on the MiScope-M2.

f. Completion of a biometric monitoring study using sweat samples and selected biomarkers

For the quantification of lactate in sweat, Person 2 always possessed the highest concentration. On most days, each individual was unique in their lactate levels, as noted by the standard deviation-based error bars on the bar graph. For the quantification of urea in sweat, the values fluctuated by day and Person 3 tends to have a higher level of urea than the other two individuals. For the quantification of L-alanine in sweat, Person 2 again tends to produce higher levels. These trends also mirrored those obtained in Objective 1 for the comparative GC-MS portion of the biometric monitoring study.

Table 4 lists the statistical p values obtained from the MANOVA and ANOVA analyses.

Table 4. MANOVA and ANOVA results for UV-Vis based metabolic analysis methods

	UV-Vis
MANOVA	p < 1.884e-15 ***
ANOVA (Lactate)	p < *2.082e-13* ***
ANOVA (Urea)	p < *3.04e-05* ***
ANOVA (Alanine)	p < *3.499e-09* ***

The p-values from the MANOVA tests for the UV-Vis data sets was calculated to be < 0.001. A low p-value supports that there is a significant statistical difference between each individual when considering the responses from all three analytes (lactate, urea, and L-alanine) together. Due to the significance of the MANOVA tests, an analysis of variance (ANOVA) test was

performed for each variable (metabolite) of the UV-Vis samples. The purpose of the ANOVA test is to establish the significance of the individual dependent variables. Each of the three ANOVA tests for the UV-Vis based analysis calculated p-values < 0.001 for each analysis. The low p-values demonstrate that there is a significant statistical difference between each individual when considering only one analyte. However, for the GC-MS based analysis, only one of the three ANOVA test, specific for lactate detection, calculated a p-valued < 0.001. Overall, the UV-Vis based analysis method proved to be a more effective method for differentiating between each individual. These statistical analyses support the ability of the set of markers together, as well as each marker separately, to distinguish individuals by UV-Vis and biocatalytic analyses.

The correlation circle of partial least squares (PLS) regression can be seen in Figure 10. This figure illustrates the correlation of the variables with the first two components associated to the first two latent variables. It is important to note that, regardless of analytical detection method (UV-Vis or GC-MS) there is a significant distance between each metabolite and as well as the day of analysis. This means that the lactate, urea, and L-alanine concentrations are not correlated with each other or with the day of analysis.

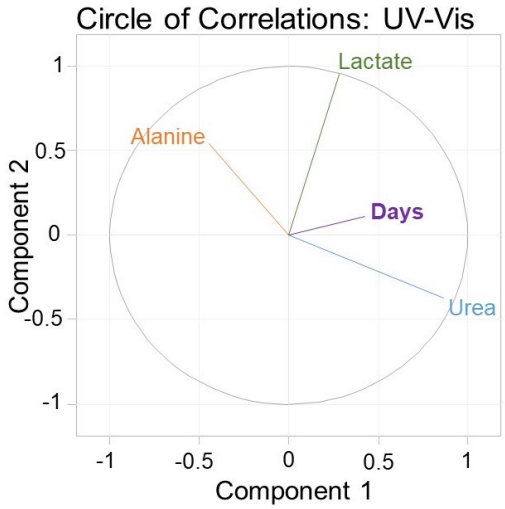

Figure 10. Correlation circle of PLS regression for the UV-Vis based analysis.

The biometric responses collected from the monitoring study were further applied towards encryption. This version of encryption builds upon our prior published work in the area[21] by focusing on the use of asymmetric encryption. Asymmetric encryption requires two keys for each person-one public and one private-in order to perform encryption. This type of encryption is used for two important aspects of cryptography: short message encryption and user authentication. This research shows that one can derive individualized keys for asymmetric encryption from a person's biometric data and successfully use these keys for both of the aspects above.

To show a proof-of-concept in this area the asymmetric cipher system to be used for these processes will be kid-RSA or kRSA, developed by Neil Koblitz.[22,23] First, the keys were generated by using the biometric data seen in Table 5 to make four values that will be used in the encryption process. The data here is seen in mM values, although for consistency of using two-digit integers, as this methodology requires integers, the values for urea were multiplied by 10. This biometric data was used to create four values to be used in the kRSA cryptosystem: M-which is used to calculate the other three, e-the public key, d-the private key, and n-which is used in both encryption and decryption. Further details of how these are calculated can be seen in Koblitz's work. These values can be seen in Table 6. The first individual is referred to as "Bob" for this

Table 5: kRSA values for Individual 1 (Bob)

M	e (public key)	d (private key)	n
2235	140848	138622	8735853

portion as "Bob" and "Alice" are the names which are used in cryptography when talking about the transmission of messages. These names have no relation to the participants.

Table 6: Biometric Data for Individual 1(Bob)

a (lactate day 1)	b (lactate day 2)	a' (urea day 1)	b' (urea day 2)
43	52	63	62

Once Bob's public key and value for n has been released, another person-here Alice-can send a secure message to Bob. Alice, or anybody who wanted to send a message to Bob, would follow the kRSA process seen in Figure 11. For kRSA, the message to be transmitted must be in Base 26. For a sample message, "HELP", the message in Base 26 is "144316" by using the cryptography version of Base 26. Alice encrypts this short message using Bob's value for e, his public key, and Bob's value for n in the following equation: ct=m·e mod(n). In this equation "ct" is the ciphertext-the encrypted text, and m is the message in Base 26. For the example message the ciphertext would become "7025890", which would correspond to "OISHN" in Base 26, showing it was truly encrypted. Once Bob receives this message, he will use his value of d, his private key, and his value for n in order to decrypt the message using the following equation: m=d·ct mod(n). The decrypted value Bob calculates then becomes "144316", correctly corresponding to the original message "HELP".

Table 7: Biometric Data for Individual 2 (Alice)

a (lactate day 1)	b (lactate day 2)	a' (urea day 1)	b' (urea day 2)
43	65	64	63

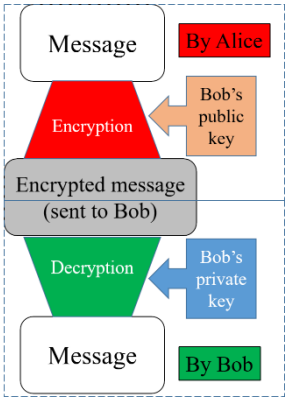

Figure 11: asymmetrical-key encryption and decryption process

A similar application to the above encryption of a message is used for user authentication via a digital encrypted signature, which can be seen in Figure 12. This process is also performed by Alice in order to show Bob that she is truly the one sending the message. Using Alice's biometric data seen in Table 4, she has her four kRSA values calculated just as Bob's were, as seen in Table 8. For her signature, "ALICE", she once again changes this to Base 26: "674055". She then encrypts this signature with her private key, d, and value for n by using the following equation: ct-m·d mod(n) resulting in a value of "6507723". This value corresponds to "NFFUA" showing that it has been encrypted. She sends this in addition to her message above to Bob. Bob would then take Alice's public key, e, and value for n in order to decrypt this signature using the following equation: m=e·ct mod(n). Bob uses this to calculate "674066, or "ALICE" which proves to him that it was truly Alice who sent that message to him.

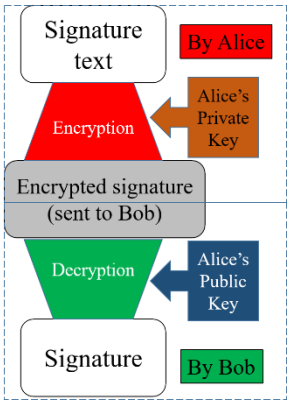

Figure 12: authentication process using asymmetric encrypted signature

Table 8: kRSA values for Individual 2 (Alice)

M	e (public key)	d (private key)	n
2794	178859	176087	11272278

2.1.3. Conclusions

a. Feasibility of determining biological sex using only one biomarker (alanine/arginine)

The results from the analysis of authentic fingerprint samples further demonstrated the ability of the bioaffinity-based ALT/POx/HRP assay to differentiate between male and female fingerprint samples based on the significant difference in absorbance intensities. The ROC/AUC analysis for the authentic fingerprints indicated a 99.8% chance of correctly identifying a male fingerprint from female fingerprint with 100% sensitivity and 96% specificity. The results from the analysis of authentic fingerprint samples using the Sakaguchi assay demonstrated the ability of the chemical assay to differentiate between male and female fingerprint samples based on the significant difference in absorbance intensities. The ROC/AUC analysis for the authentic fingerprints indicated a 100% chance of correctly identifying a male fingerprint from female fingerprint with 100% sensitivity and 100% specificity. Since the mimicked samples and the authentic samples produced the same ROC/AUC values, two conclusions can be drawn. The first is that there is minimal, if any, interference from the other compounds known to be in fingerprints that would otherwise cause a matrix effect. The second possibility is that the Sakaguchi test is superior in sensitivity to other methods thus indicating that any sample matrix is "overlooked" by the method.

b. *Lactate, urea, and glutamate quantification for biometric purposes*
The results generated by this study demonstrate the collective ability of compounds inherent in sweat to differentiate individuals based on person-specific metabolic concentrations. The three biocatalytic assays presented in this manuscript have proven to be reliable and reproducible for distinguishing individuals from one another based on the concentrations of lactate, urea, and glutamate for each mimicked and authentic sweat sample. The successful development of these three assays gives us three more potential markers that can ultimately be used to determine information about a person that leaves behind his/her sweat, which is a major compound of fingerprints.

c. *Optimizing our currently developed fingerprint extraction method*
The results generated by this study demonstrate that the efficacy of the extraction protocol is largely dependent on the assay that will ultimately be used for the detection of the amino acids extracted from the fingerprint sample. From these studies, it was determined that when using the ninhydrin assay, HCl pH 1.06 had the optimal response. However, when using the Bradford assay, the original method proved to have the optimal conditions since changing the pH shifted the λ_{max} out of the acceptable range. Following this modification, both chemical assays were used to assess the extraction protocol when using three pHs of acetic acid (pH 2.04, pH 3.03, and pH 4.05) instead of HCl. For both assays, acetic acid did not show any improved response. As such, for the final modification – the addition of Tween 20 –HCl pH 1.06 and 10 mM (pH 2.15) were used with the ninhydrin assay and only 10 mM (pH 2.15) was used with the Bradford assay. For this modification, the addition of Tween 20 significantly decreased the efficacy of the extraction. Ultimately, after all three modifications were completed, it was determined that when using the ninhydrin assay, HCl pH 1.06 without Tween 20 contained the ideal conditions and for the Bradford assay, 10 mM HCl (pH 2.15) without Tween 20 possessed the ideal conditions. The most likely cause of the difference in HCl needed is due to the fact that the Bradford reagent is pH sensitive as indicated in literature.

d. *Evaluating how time since deposition (TSD) can affect our fingerprint samples*

There is a well-defined, decreasing trend along the 12 weeks of aging for all three methods of analysis. All three chemical assays were determined to be capable of differentiating between an aged female fingerprint and a fresh male fingerprint for up to 84 days. At the end of this study, the aged female samples were beginning to provide responses close to that of a fresh male sample but could still possibly make this differentiation with time points past the 84 days.

e. Ketone Body monitoring in sweat

The results of this project have proven to be favorable for the development of a sensing concept for ketone bodies in a person's sweat. This concept has particularly high value for those who have been diagnosed with diabetes in order to help prevent the harmful and sometimes life-threatening effects of ketoacidosis. Here, it has been demonstrated that there is a direct correlation between the concentration of β-HB and the ΔAbs. at both 340 nm from the production of optically inactive NADH via NAD^+ and βHBDH and at 580 nm from the production of formazan dye upon reduction of NBT via NAHD and PMS. The PMS/NBT step is vital to this concept as it is the only way to generate an optically active compound. Based on these results, it was confirmed that the amount of formazan dye produced is directly proportional to the concertation of β-HB in the original sample. Furthermore, the imaging step used to but a numerical value to these results was proven successful, in that the mean gray value was demonstrated a direct, linear correlation to the Blue Nile A dye standard as well as the concentration of β-HB. Furthermore, these results were confirmed regardless of if the camera used was from a smartphone or a portable microscope. This provides substantial support to the concept of developing a wearable strip/patch which can be analyzed using a smartphone.

f. Completion of a biometric monitoring study using sweat samples and selected biomarkers

This work demonstrates the collective ability of compounds inherent in sweat to differentiate individuals based on his/her person-specific metabolic concentrations over an extended time period. The MANOVA test demonstrated the combined ability of three metabolites in sweat to distinguish between three individuals; using both the UV-Vis based and the GC-MS based analytical methods. The UV-Vis responses provided more distinguishing power than the GC-MS when considering both the MANOVA and ANOVA tests. The correlation circles of PLS regression further demonstrate that each individual possesses their own unique combination of all three metabolites that is not dependent on time, and could be monitored effectively for biometric purposes. Future work will focus on finding and evaluating additional markers to add to this panel. After establishing identity, we will aim to look at each developed system for correlations to personal attributes, such as age, food habits, and ethnicity.

The process of encryption explored here, using biometrics as building blocks used to derive keys instead of using them as keys, is a promising methodology in order to alleviate this issue. Seen here, one is able to both encrypt and decrypt a short message with keys derived from biometric data and also to use biometrically-derived keys in order to produce an encrypted digital signature for user authentication. As these are the two uses for asymmetric ciphers, this is a worthwhile endeavor for the future of cryptography and biometric authentication. It is important to note that for this to be more viable, a long string of biometric data would need to be used instead of the two-digit integers seen here, possibly hundreds of digits long.

3. Objective 3: *Development of field-deployable (on-site) applications using the established bioaffinity-based systems*

Summary

We have worked towards the development of field deployable devices for the detection and quantification of both ethanol and marijuana use. This objective has focused on the development of a field-deployable paper strip for an on-site method of analysis for ethanol found in fingerprints and sweat of active drinkers. Additionally, a compatible smartphone application has been produced capable of quantifying the amount of color on the paper substrate. Initial population studies have begun and are outlined in this objective.

3.1.1. Experimental work

Ethanol Detection

This assay uses the enzymes alcohol oxidase (AOx; E.C. 1.1.3.13) and horseradish peroxidase (HRP, E.C. 1.11.1.7) as well as ABTS dye to convert ethanol within a sample into a visible color change that is blue-green. This system is realized on filter paper using potassium phosphate buffer pH 7.6 containing 100 mU AOx, 10 U HRP, and 10 mM ABTS.

Camera Based Calibration on Filter Paper

The described enzymatic cascade was developed on filter paper using a range of ethanol standards. Filter paper was chosen for its color, which served as a suitable platform and background for the imaging process. The ethanol standards were prepared at the molar equivalents of anticipated blood alcohol concentrations in drinking individuals. This range consisted of 0 % BAC to 0.25 % BAC (0 mM to 54.23 mM ethanol). Due to the sensitivity of this assay, as little as 10 µL of each sample was required for analysis. For each piece of filter paper, 10 µL of deionized water was deposited on the left side (control) and 10 µL of the equivalent ethanol concentration was deposited on the right side (sample). Immediately afterwards, 10 µL of a prepared reaction mixture containing 100 mU AOx, 10 U HRP, and 10 mM ABTS was added to each deionized water and ethanol spiked area. When ethanol is present, the product will develop a blue/green color. This color is proportional to the amount of ethanol present. Figure 13 demonstrates an example of the spiked filter paper compared to a negative control.

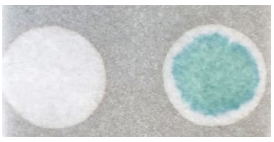

Figure 13. Filter paper system imaged with the document camera after 3 minutes of analysis. The control (left) is DI water and the sample (right) is an 0.08 % BAC ethanol sample.

Images were taken of the calibrated ethanol samples with both the document camera and the Android smartphone camera after 3 minutes of reaction time. Images from the document camera were analyzed using Fiji (Image J) to determine the mean gray values. The developed smartphone application calculated the mean gray values for the images taken with the Android camera. In order to correct for the differences in the white balancing of the photos, the mean value of the deionized water area was subtracted from the ethanol area on each piece of filter paper. The absolute values of the corrected mean gray values were used for the calibration curves.

$$\text{Corrected Mean Gray Value} = \text{ABS}(\text{Mean Gray Value of Sample} - \text{Mean Gray Value of Control})$$

With this method, the average and standard deviation of the corrected mean gray values were calculated for each sample and plotted against concentration. This platform allows for colors visible by naked eye to be qualitatively and quantitatively visualized by both the document camera and the smartphone application.

Development of a Smartphone Application

During the development and optimization of the filter paper based reaction system, a compatible smartphone application was simultaneously created by Michael McDaniel. The development of this smartphone application was carried out using the Android Studio Integrated Development Environment (IDE)[24] along with Java programming language. The IDE provided the ability to interface with smartphone hardware including the screen and camera, and provided the ability to present a Graphical User Interface (GUI) to the user to control the application. A prototype application has been created that allows the user to capture photographs and provide the user with information about the colors in selected regions for use in collecting measurements. This application has the ability to capture photographs of the filter paper system and provide the user with a calculated BAC for comparison to the standard breathalyzer response, as depicted in Figure 14.

Figure 14. A screenshot of the smartphone application while collecting the mean gray value information from a photograph.

The color of an object captured by a smartphone camera may be affected by the lightning conditions or the device's built-in white-balancing. These factors may vary based on the smartphone manufacturer. Therefore, it is necessary to determine what these lighting conditions are and to correct for them when measuring color. The lighting conditions were determined by taking an image of a known color standard and evaluating how it has been affected. An algorithm was devised that uses the information from the control color appearance to correct for the lighting's distorting effect on the sample. The normalized color will be used to determine the corresponding BAC through a pre-programmed calibration curve containing color information for a range of known ethanol concentration ranges.

Controlled Drinking Study and Prototype Trial

In order to evaluate the ability of the developed enzymatic system to function on filter paper with subsequent analysis using the smartphone application, ten active drinkers provided sweat samples during a controlled drinking study. A 0.4% pilocarpine nitrate solution and a 0.07 N sodium bicarbonate solution were applied to the positive and negative electrodes, repectively. The forearm of each volunteer underwent iontophoresis for 10 minutes. Afterwards, sweat was collected into a clean, dry gauze pad which was placed on the iontophoresized skin, covered with a polyethylene square and secured with waterproof adhesive tape. After a 30 minute collection period, the gauze pad was collected and centrifuged to collect the produced sweat.

Each volunteer first provided a sober sweat sample with a breathalyzer response of 0.000% BAC. After collection of this sample, each volunteer consumed three consecutive 44 mL servings of 40 % vodka (totaling 132 mL). The BACtrack S80 breathalyzer was used to monitor changes in blood alcohol concentration. A breathalyzer reading was taken before, during, and after sweat collection via pilocarpine iontophoresis. The average of these breathalyzer readings were compared to the assay response with the collected sweat sample. Volunteers provided a total of three sweat samples, resulting in a sober sample, a high BAC % sample, and a low BAC % sample. All samples were handled accordingly to prevent cross-contamination. In total, ten volunteers supplied a total of 30 sweat samples for analysis, which were each analyzed in triplicate. A sample volume of 10 µL was used to mirror the calibration curve. On each day of analysis, the calibration curve was repeated alongside the samples. This allowed for the sweat ethanol concentrations to be calculated for each sweat sample. An example of the assay in action is depicted in Figure 16.

Statistical Analysis

This study was designed to compare the filter paper based enzymatic system's ability to correlate sweat alcohol concentration to the breathalyzer response of the active drinkers in the controlled drinking study. For each sample collected and analyzed in the controlled drinking study, a calibration curve was used to calculate the relative BAC of each sweat sample. Statistical analysis was implemented to compare the average breathalyzer response of each sample to the sweat alcohol concentrations that were calculated using the smartphone application. The Pearson coefficient was calculated to evaluate the correlation between the average breathalyzer responses and the average sweat alcohol concentrations. The value of a Pearson coefficient can range from -1 to 1, where[25] Pearson coefficients ranging from 0.7 to 1 are considered to be highly correlated in a positive and linear fashion.

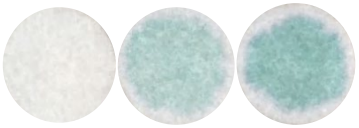

Figure 15. Images of the filter paper system using sweat collected from a volunteer in the controlled drinking study after 3 minutes reaction time. The BAC % from the breathalyzer for each sample is 0.000%, 0.058%, and 0.079% from left to right. There is an increase in color intensity as the breathalyzer response increases.

THC Detection

Preparation and Use of the Sensing Surface

For the THC metabolite detection concept, a competitive immunoassay was employed. The three buffers exclusively used throughout this process were 1X phosphate buffered saline (PBS) pH 7.5, 0.1 M carbonate buffer pH 8.5, and 0.1 M citrate buffer pH 5.5. All solutions of the antibody and the antigens were prepared fresh daily. Preparation of the sensing surface was a two-day process and utilized ultra-high binding 96-well microtiter plates. Figure 16 provides a general description of the steps involved in preparing the sensing surface. The first step employed a 1-hour, room temperature incubation of a 1 % poly(ethyleneimine) solution (PEI). This was followed by three washes (3x) with ultrapure water. Next a 1 % latex polystyrene bead solution was incubated for 3 hours at 4 ˚C, followed by another set of three washes with ultrapure water. The final step of day one's preparation involved an overnight incubation at 4 ˚C of 1 µg/mL anti-THC antibody. To begin the second day of preparation, the wells were washed 3x with PBS buffer and then blocked for 1 hour at room temperature with a 1 % BSA solution. The wells were washed again 3x with PBS buffer and the final preparation step commenced with a 1-hour, room temperature incubation of either THC-HRP alone or a mixture of both THC-HRP and THC-COOH, depending on the experiment being conducted. For optimization of the sensing platform (THC-HRP alone), the conjugate was diluted 750 times (750x), 500 times (500x), and 250 times (250x) in PBS buffer. The wells were washed three final times with PBS buffer before analysis via the horseradish peroxidase (HRP) assay. Figure 17 displays a visual representation of the immunoassay construct solely using the THC-HRP. This construct results in the maximum response of the assay as there is no metabolite present to induce competition. Also

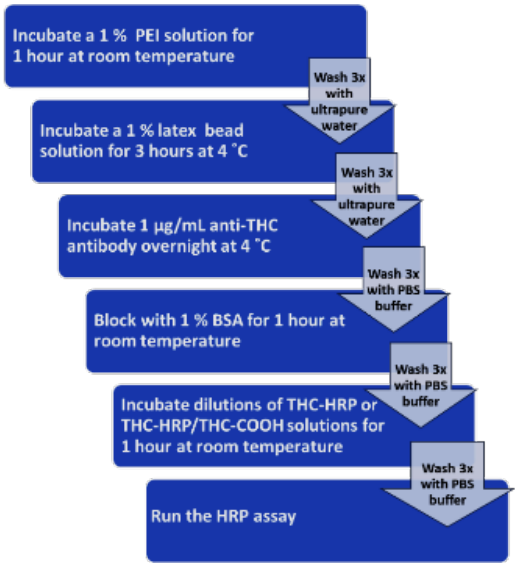

Figure 16. Summary of preparation steps for the immunoassay sensing surface.

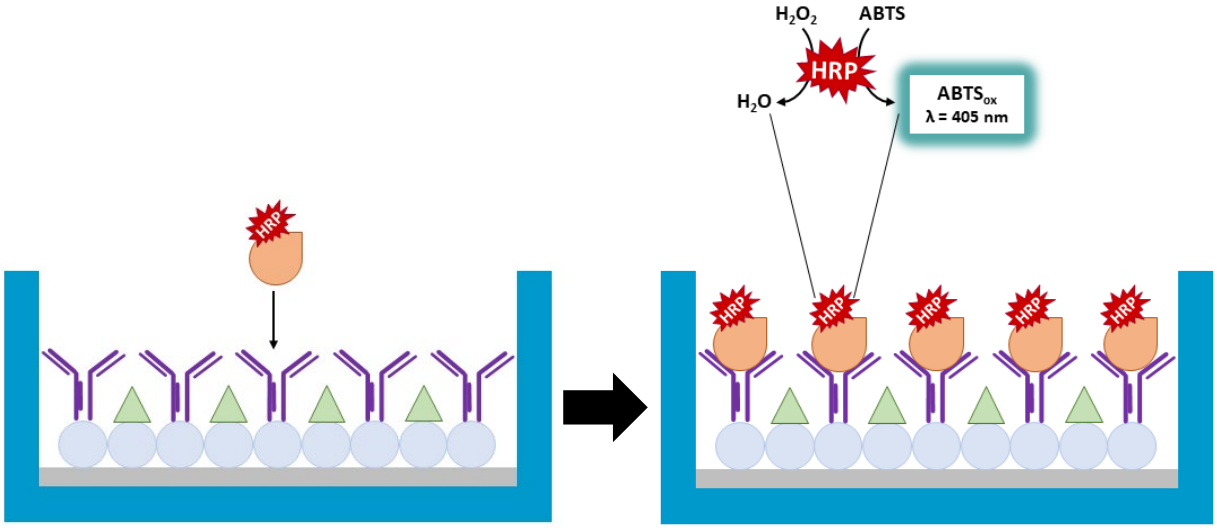

Figure 17. Depiction of the final and accepted attempt at an immunoassay construct with antigen only. The blue "U" shape represents the microtiter well, the gray bar represents the PEI, the blue circles represent the latex beads, the green triangles represent BSA, the purple "Y" shape represents the anti-THC antibody, and the orange teardrop shape represents the THC antigen labeled with HRP. The schematic of the HRP assay is also depicted on the right, where HRP bound to the antibody oxidizes ABTS in the presence of H_2O_2 to produce a blue-green color that is measured spectrophotometrically at 405 nm.

shown here is the scheme for the HRP assay, which utilizes the HRP bound to the sensing platform along with and a bulk solution containing 1 mM ABTS, 1 mM H_2O_2 and citrate buffer. Once these reagents are mixed, the H_2O_2 oxidizes the ABTS dye to produce a visible blue-green color that can be measured spectrophotometrically at 405 nm.

Final Calibration Curve

Following the determination of the detection window for this sensing system, it was important to narrow in on a more accurate range. This would provide the platform needed to target THC-COOH in real fingerprints. Furthermore, the narrower the range that can be detected, the

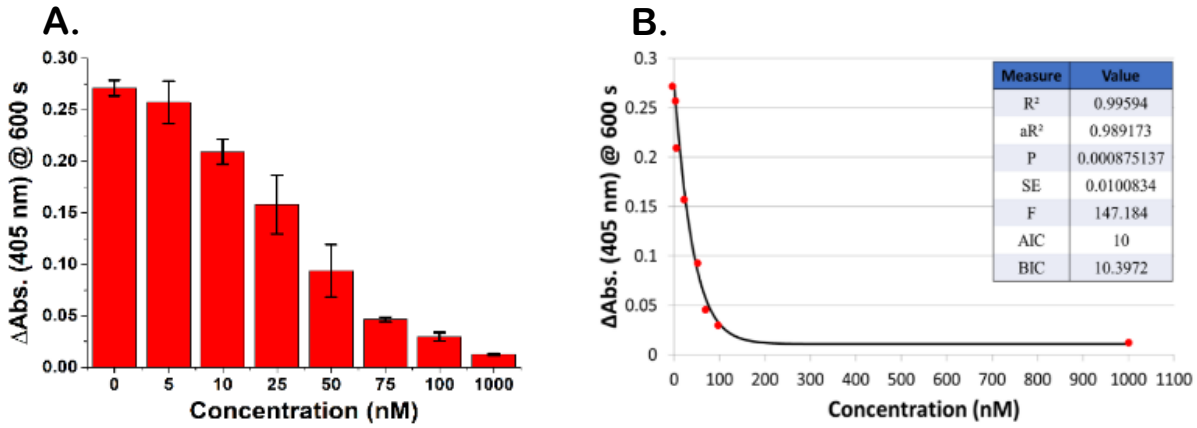

Figure 18. (A) Response from buffer-based THC-COOH samples (n=3) following 600 s of analysis and (B) fitted with a five-parameter logistic (5PL) curve.

more likely this system could be used in parallel to legal regulations in the future. The data previously collected provided substantial evidence that the threshold for detection of THC-COOH with this competitive immunoassay is actually between 5 nM and 1000 nM. This calibration curve included the following concentrations: 1000 nM, 100 nM, 75 nM, 50 nM, 25 nM, 10 nM, and 5 nM. This new range resulted in a much clearer differentiation between these concentrations which can be seen in Figure 18A. These results indicated that the competitive immunoassay paradigm that was created is sensitive enough to differentiate a narrow window of concentrations, as well as detect minute concentrations that may be present in the sweat secretions of a THC user. Additionally, this final calibration curve determined that the detection boundaries for this sensing system were 5 nM on the low end and 100 nM on the high end. While 1000 nM is still detectable, it may not be practical for actual use given its significantly low response. To further support this data, this calibration curve was fit with a 5 parameter logistic (5PL) nonlinear regression, Figure 18B, which is typically used for asymmetrical data such as that generated by immunoassay.[26-29] The R^2 value for this calibration curve is 0.993 which indicates a good fit. This confirmation provided the confidence needed to move forward with real fingerprints.

3.1.2. Significant Results

Alcohol Study

Camera Based Calibration on Filter Paper-Comparison between the Document Camera and Smartphone Application

The results of the ethanol calibration on filter paper that were evaluated using the Android camera and smartphone application is shown in bottom graph of Figure 5. As seen in the filter paper images for each concentration, as the BAC % increases, the intensity of the color produced also increases.

These results exhibit the dependence of the visible color change with the amount of ethanol in the system. The linear response shown by the ethanol standards that were visualized by the smartphone camera and application are very similar to the same ethanol standards visualized by the document camera and Fiji (Image J). To further evaluate the two methods of visualization, Figure 20 was created using the corrected mean gray values from the ethanol calibration.

The Pearson's correlation of this plot is 0.995 and is indicative of a strong, linear relationship between the two visualization systems. This comparative analysis demonstrates the ability of the developed, portable alcohol biosensor and both visualization systems to quantify ethanol concentration based on the color produced after three minutes. Based on the comparable results between the two visualization methods, the smartphone application alone was used for the remaining studies. This work aims to establish the ability of the developed alcohol biosensor and corresponding smartphone application to quantify sweat alcohol concentrations in active drinkers.

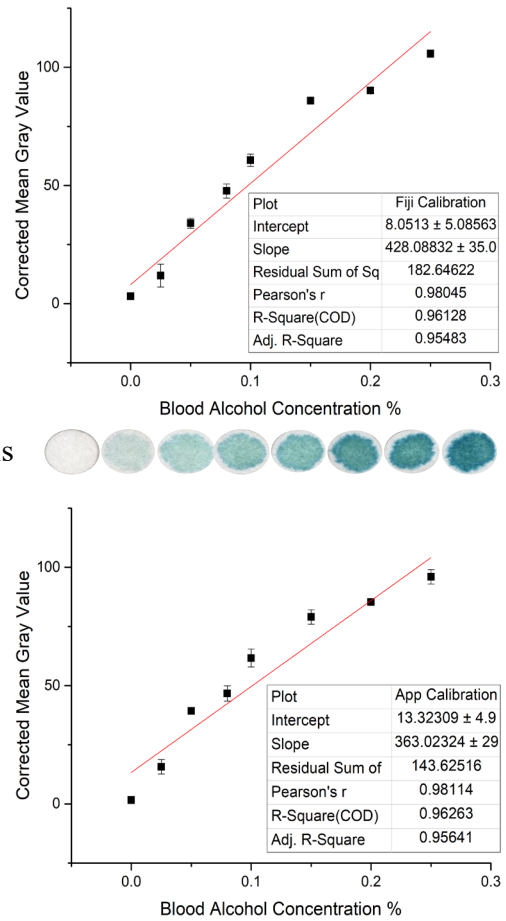

Figure 19. A calibration curve between the mean gray value and blood alcohol concentration using ethanol standards with the filter paper system after 3 minutes. The top graph was created using the document camera images and analyzed with Fiji (Image J). The filter paper images from the document camera are shown between each graph and represent each ethanol concentration. The bottom graph was created using the Android camera images that were analyzed with the smartphone application.

Controlled Drinking Study and Prototype Trial

Ten volunteers participated in a controlled drinking study and supplied three sweat samples each at different BAC %. The extracted sweat samples were directly applied to filter paper and reacted with the enzymatic mixture. Images were taken with an Android smartphone camera and evaluated using the developed smartphone application. To determine if the average breathalyzer responses from each sweat collection were well correlated to the enzymatic cascade response with sweat, the correlation plot in Figure 20 was created. This figure shows the correlation between blood alcohol percentage from the breathalyzer responses and the calculated sweat alcohol concentration of each sweat sample. The Pearson's coefficient is 0.88, which is indicative of a strong, positive relationship between

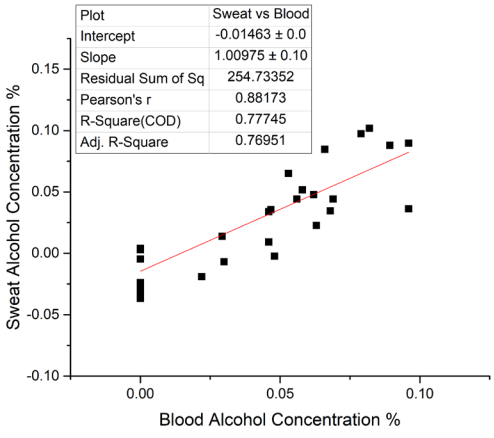

Figure 20. Calculated sweat alcohol concentrations per sample collected compared to breathalyzer determined BAC %.

breathalyzer response and sweat alcohol concentration calculated using the developed smartphone application. This portable system is capable of quantifying the amount of ethanol in the authentic, human sweat of ten different individuals who participated in the controlled drinking experiment when compared to the breathalyzer responses.

THC Study

The initial experiments for this research focused on developing a sensing surface suitable for detecting low concentrations of THC-COOH, one of the main metabolites present after the use/consumption of THC. Following optimization, it was decided that 1 µg/mL anti-THC antibody was suitable for this for methodology. Additionally, it was determined that a combination of 1 % PEI and 1 % latex polystyrene beads was necessary for enhancing the binding of the anti-THC antibody to the microtiter plate surface. Following this development, the next step was to determine the appropriate amount of conjugated THC-HRP needed. With THC-HRP being an expensive compound, it was important to balance cost and assay efficacy. To do this, THC-HRP dilutions of 750x, 500x, and 250x, prepared in PBS buffer pH 7.4, were used. Despite wanting to use a more dilute solution to reduce the amount of material needed, these results confirmed that the 250x dilution was the optimal concentration of THC-HRP, as it generated a much-improved assay response as compared to the other dilutions.

Spiked Fingerprint Samples

The first step toward utilizing this sensing platform as a roadside method for the detection of THC metabolites was to introduce the fingerprint/sweat matrix to the immunoassay to ensure it did not compromise the response shown by the buffered samples. A modified extraction protocol was also established since THC-COOH would not be extracted by the typical aqueous 10 mM HCl protocol. As such, methanol was used. Following the procedure outlined above, a volunteer who had disclosed they do not use THC products provided fingerprints. These samples were then spiked with the various concentrations of THC-COOH prior to the first vortex step in order to mimic its presence as a metabolite in the fingerprint secretions from actual THC users. As shown in Figure 21A, there is a decreasing trend generated as the concentration of THC-COOH is increased due to the binding competition between the THC-COOH metabolite and the THC-HRP conjugate which is responsible for the color production. Because the antibody has a greater affinity for the metabolite, if present, it will bind more readily than the THC-HRP. As seen, there is a noticeable decrease in the overall response of the system. This can be attributed to the presence of the fingerprint/sweat matrix, as indicated by the bars at 0 (1) and 0 (2) which represented samples with no THC-COOH/no fingerprint and no THC-COOH/with a fingerprint, respectively. Ultimately, this caused the separation between individual concentrations to be less defined as compared to the buffered samples. Despite this, the concentrations between 5 nM and 100 nM were still be detected and differentiated.

The data from this analysis was fit with a 5PL nonlinear regression and is illustrated in Figure 21B. This generated an R^2 of 0.998, indicating a good fit and supported the observation that it is possible to detect nanomolar concentrations of THC-COOH even in the presence of the fingerprint/sweat matrix. The success of this experiment using authentic fingerprints spiked with

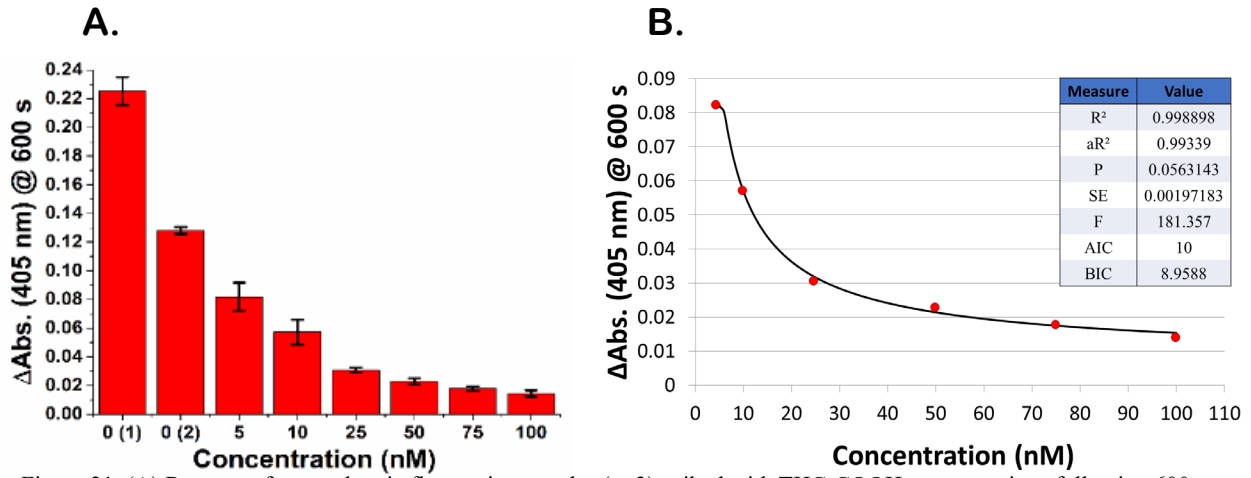

Figure 21. (A) Response from authentic fingerprint samples (n=3) spiked with THC-COOH concentrations following 600 s of analysis and (B) fitted with a five-parameter logistic (5PL) curve. The bars at 0 (1) and 0 (2) represent the blank samples for this experiment – no THC-COOH/no fingerprint and no THC-COOH/with a fingerprint, respectively.

THC-COOH concentrations provided a substantial foundation for the next step, which was to use real fingerprint samples from individuals who had actively used a THC-containing product, specifically marijuana. Given the range of metabolite detection that is seen here, there is evidence that the response of this type of system has the potential to be correlated to legislative levels regarding impairment.

Fingerprints Analysis of Real THC Users versus Non-Users

Ultimately, fingerprints from individuals who were actively high were collected and compared to those collected from individuals who were considered non-users (those who had not consumed THC-related products in 30 days or more). In addition, fingerprints from each active user were collected prior to the use of marijuana as control samples. Two sets of fingerprints were also collected from non-users in order to show that collection time did not have a role in the data generated by the assay. All second sets of fingerprints were collected 30-75 minutes apart due to the practical availability of the volunteer and the collector.

On the left (Figure 22A) are the responses from marijuana users. As shown, when the users were actively high, the response of the system decreased as compared to their sober fingerprints. On the right (Figure 22B) are the fingerprints from non-users. In both cases, the blank sample corresponds to samples that contain only THC-HRP (no fingerprint/no THC-COOH). As shown, there is no difference between the fingerprints collected first (T1) or those collected second (T2), indicating that the time between collections was not a contributing factor to the difference in responses. Also, the error shown in both figures indicates that the extraction process was reliable for removing THC-COOH from within the fingerprint/sweat content. Furthermore, these results clearly demonstrate the immunoassay construct developed and optimized here can determine

whether or not someone has used a THC-related product using the metabolites present in their fingerprints. Further studies on this topic are ongoing in our research lab.

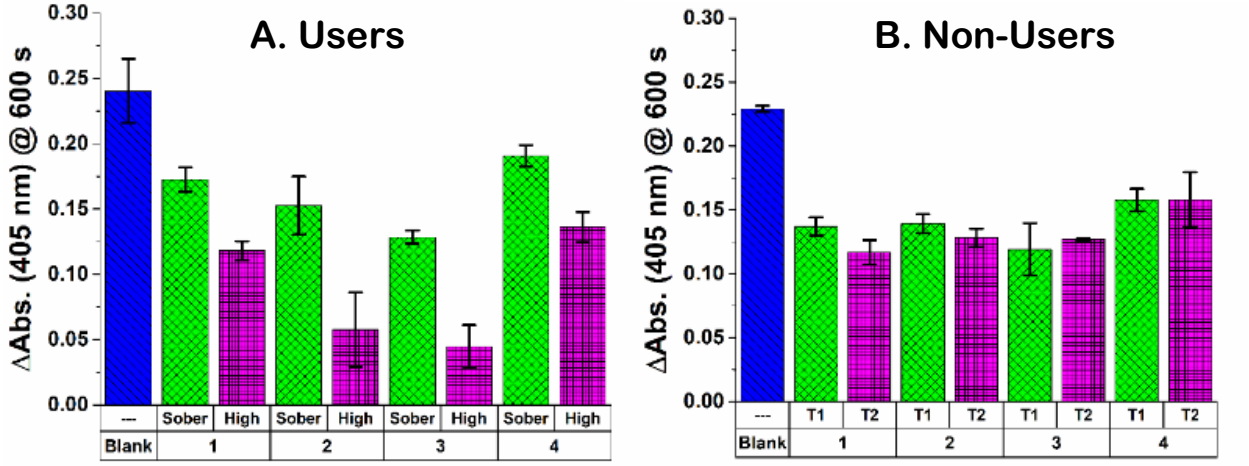

Figure 22. Response from authentic fingerprints (n=3) following 600 s of reaction time from (A) active marijuana users and (B) non-users. The abbreviations for this figure include T1 and T2, which represent the two time points used for collection of fingerprints from non-users ranging from 30-75 minutes. The single numbers on the bottom axis represent the volunteer number. The blank sample consists of THC-HRP with no fingerprint/no THC-COOH.

3.1.3. Conclusions

Ethanol

A portable, enzymatic system has been developed on filter paper with a corresponding smartphone application capable of quantifying the amount of ethanol present in sweat with a smartphone application. The sweat collected from ten individuals demonstrates a positive, linear relationship between blood and sweat alcohol concentrations after three minutes of reaction time.[6] This system does not require complex instrumentation and its portability allows for future field use and commercialization. As a commercial product, this research introduces a single-use system that offers affordability and intuitive user handling.

This research required sweat production to be stimulated through pilocarpine iontophoresis in order to collect adequate sample volumes for triplicate analyses. Although the feasibility and applicability of the developed system to be used commercially has been established, this product would benefit from continued research into the evaluation of resting sweat rates and lower sample volumes. Additionally, the reaction enzymes and substrates will need to be stabilized onto the portable surface and their stability evaluated before starting any in-field trials. Future developments could provide a portable system similar to a pregnancy test or pH paper with a compatible smartphone application that could report blood alcohol concentrations based on sweat content in a matter of minutes.

THC

In summary, a simple and sensitive protocol for the detection of the THC-metabolite, THC-COOH, has been developed. Since there is limited knowledge of THC-COOH in sweat as well as the fact that currently there is a zero-tolerance policy for operating machinery/vehicles under the influence of THC, the research presented here was centered on detection of THC-COOH, rather than quantification. This protocol is capable of detecting as little as 5.0 nM THC-COOH and as

much as 100 nM THC-COOH, in addition to the ability to differentiate between a narrow window of concentrations.

Fingerprints from active THC users – specifically individuals who used marijuana – were utilized. These samples were also compared to non-users. The results of this research indicated that when individuals were actively high, the absorbance of immunoassay decreased as compared to the response from their sober control samples. These results confirmed that it is possible to determine if a person has used THC-containing products from the sweat content of their fingerprints.

The goal of this research was to find a fast and effective way to detect THC metabolites in a person's system in order to someday provide law enforcement with an on-site method for determining use of THC-products such as marijuana, similar to a breathalyzer. Due to the nature of this immunoassay construct presented here, it can be readily combined with a strip-like design – like that of a pregnancy test or glucometer – which would provide law enforcement with a method that requires little to no scientific training.

This methodology has the potential to parallel legal legislation regarding acceptable limitations for operating machinery and driving. Ultimately, this research could also be applied to all illicit substances and drugs of abuse due to the sensitive, flexible, and straightforward nature of the competitive immunoassay coupled with an optical readout.

Dissemination to Communities of Interest

The results have been disseminated in several conferences as oral and poster presentations since the awarding of this grant. Since the start of this grant, members of the Halamek Lab have participated in many conferences and meetings both regional and national. These include the 252nd American Chemical Society (ACS) National Meeting & Exposition in August 2016, 41st Northeast Regional Meeting (NERM) in October 2016, 42nd Annual Meeting of the Northeastern Association of Forensic Scientists (NEAFS) in October 2016, 69th Annual Scientific Meeting of the American Academy of Forensic Sciences in February 2017, the 9th Annual Eastern New York American Chemical Society's Undergraduate Research Symposium in April 2017, 253rd ACS National Meeting & Exposition in April 2017, the 21st Triennial Meeting of the International Association of Forensic Sciences (IAFS) in August 2017, and the 43rd Annual Meeting of the Northeastern Association of Forensic Scientists (NEAFS) in November 2017, the 70th Annual Scientific Meeting of the American Academy of Forensic Sciences in February 2018, the Pittcon Conference and Expo in February 2018, the Pittcon Conference and Expo in March 2019 and the Northeastern Regional Meeting (NERM) in June 2019. We have published three different research projects encompassing non-invasive alcohol and THC detection, as well as introducing our concept for encryption. From these publications, our research has received media attention from several scientific news journals and the local news channels.

Mindy Hair has defended and published her dissertation entitled, "Bioaffinity-based Methods for Biometric, Forensic and Clinical Purposes." Due to the quarantine and restrictions imposed from COVID-19, future conference travel has been suspended.

II. PRODUCTS

Publications

Huynh, C.; Brunelle, E.; Agudelo, J.; Halámek, J. Bioaffinity-based assay for the sensitive detection and discrimination of sweat aimed at forensic applications. *Talanta*, 2017, 170, 210–214.

Brunelle, E.; Huynh, C.; Alin, E.; Eldridge, M.; Le, A.-M.; Halámková, L. ; Halámek, J. Fingerprint Analysis: Moving toward multi-attribute determination via individual markers. *Anal. Chem*. 2018, 90, 980–987.

Hair, M.; Mathis, A.; Brunelle, E. ; Halámková, L. ; Halámek, J. Metabolite biometrics for the differentiation of individuals. *Anal. Chem.* 2018, 90, 5322-5328.

McGoldrick, L.; Weiss, E.; Halámek, J. Symmetric-key encryption based on bioaffinity interactions. *Synth. Bio. (ACS)* 2019, 8 (7):1655-1662.

Hair, M.; Gerkman, R.; Mathis, A.; Halámková, L.; Halámek, J. Noninvasive concept for optical ethanol sensing on the skin surface with camera-based quantification. *Anal. Chem*. 2019, 91, 24, 15860-15865.

Brunelle, E.; Thibodeau, B.; Shoemaker, A.; Halámek, J. Step toward roadside sensing: noninvasive detection of a THC metabolite from the sweat content of fingerprints. *ACS Sens.* 2019. https://pubs.acs.org/doi/abs/10.1021/acssensors.9b02020

Submitted:
McGoldrick, L.; Halámek, J. AES encryption utilizing bio-recognition paradigm.

Hair, M.; Gerkman, R.; McDaniel, M.; Halámková, L.; Halámek, J. Non-invasive quantification of sweat glucose for health monitoring by wearable electronic devices.

Brunelle, E.; Thibodeau, B; Eldridge, M.; Halámková, L.; Halámek, J. Determination of the time since deposition of fingerprints.

Eldridge, M.; Hair, M.; Halámková, L.; Halámek, J. Differentiation of sweat samples via biomarkers with parallel enzyme cascade and GC-MS analysis.

Presentations

The research regarding the noninvasive alcohol project and the biometric monitoring has been presented by Mindy Hair in her dissertation. See above list of conferences attended for further dissemination.

Media

The Halamek Group has maintained a website that is currently under the process of relocation. On this webpage will be links to our various publications, media coverage, biographies of our members and outreach efforts. Listed below are several media highlights from papers affiliated with the grant funding.

Step toward roadside sensing: noninvasive detection of a THC metabolite from the sweat content of fingerprints

- Phys.org: https://phys.org/news/2020-01-forensic-chemist-marijuana-use-based.html

- Forensic Magazine: https://www.forensicmag.com/559618-Roadside-Sweat-Test-Can-Detect-Marijuana-Use/
- Laboratory Equipment: https://www.laboratoryequipment.com/559647-Tests-Use-Sweat-to-Reveal-Alcohol-Marijuana-Use/
- Engineering 360: https://insights.globalspec.com/article/13269/forensic-chemist-develops-marijuana-detecting-test-strip-for-law-enforcement
- New Medical Life Sciences: https://www.news-medical.net/news/20200106/New-sweat-test-could-help-detect-a-persone28099s- marijuana-use.aspx
- Marijuana Today: https://www.mjtoday.org/2020/01/new-sweat-test-to-detect-marijuana.html

Noninvasive concept for optical ethanol sensing on the skin surface with camera-based quantification

- Phys.org: https://phys.org/news/2019-12-forensic-chemist-breathalyzer.html
- Popular Mechanics: https://www.popularmechanics.com/technology/security/a30209412/drunk-sweat/
- Forensic Magazine: https://www.forensicmag.com/559138-Sweat-testing-Strip-Could-Be-Breathalyzer-s-Replacement/
- Laboratory Equipment: https://www.laboratoryequipment.com/559647-Tests-Use-Sweat-to-Reveal-Alcohol-Marijuana-Use/
- Press Reader: https://www.pressreader.com/usa/albany-times-union/20200106/281535112919708
- Center for Technology and Behavioral Health: https://www.c4tbh.org/your-sweat-can-give-away-how-drunk-you-are/
- New technology and Science News: https://newatlas.com/science/sweat-test-strips-breathalyzers/

Metabolite biometrics for the differentiation of individuals.

- Forensic Magazine: https://www.forensicmag.com/news/2018/04/sweat-could-distinguish-between-individuals-crime-scene
- Digital Journal: http://www.digitaljournal.com/tech-and-science/science/chemist-uses-sweat-analysis-to-identify-individuals-at- crimes/article/521335
- Phys.org: https://phys.org/news/2018-05-forensic-chemist-distinguish-individuals-crime.html
- Times Union: https://www.timesunion.com/local/article/Your-sweat-can-reveal-your-gender-University-at-12901529.php
- The Verge: https://www.theverge.com/2018/5/14/17352044/sweat-science-health-biomarkers-forensics

- IFL Science: http://www.iflscience.com/chemistry/this-new-technique-could-identify-suspects-at-a-crime-scene-in-just-30- seconds/
- The Verge: https://www.theverge.com/2018/5/14/17352044/sweat-science-health-biomarkers-forensics
- The Tribune: http://www.tribuneindia.com/news/sweat-at-crime-scene-may-help-nab-criminals/585160.html

Other recognition

- C&EN (American Chemical Society): https://cen.acs.org/analytical-chemistry/forensic-science/Fingerprints-just-patterns-re-chemical/97/i10
- Phys.org: https://phys.org/news/2019-03-fingerprints-revisited.html

III. PARTICIPANTS & OTHER COLLABORATING ORGANIZATIONS

Participants

Name:	Mindy Hair
Project Role:	Graduate Student
Nearest person month worked:	42
Contribution to Project:	No change
Funding Support:	None
Collaborated with individual in foreign country:	N/A
Country(ies) of foreign collaborator:	N/A
Travelled to foreign country:	N/A
If traveled to foreign country(ies), duration of stay:	N/A

Name:	Morgan Eldridge
Project Role:	Graduate Student
Nearest person month worked:	12
Contribution to Project:	No change
Funding Support:	None
Collaborated with individual in foreign country:	N/A
Country(ies) of foreign collaborator:	N/A
Travelled to foreign country:	N/A
If traveled to foreign country(ies), duration of stay:	N/A

Name:	Leif McGoldrick
Project Role:	Graduate Student
Nearest person month worked:	12
Contribution to Project:	No change
Funding Support:	None
Collaborated with individual in foreign country:	N/A
Country(ies) of foreign collaborator:	N/A
Travelled to foreign country:	N/A

If traveled to foreign country(ies), duration of stay:	N/A

Name:	Jan Halamek
Project Role:	Principal Investigator
Nearest person month worked:	21
Contribution to Project:	No change
Funding Support:	None
Collaborated with individual in foreign country:	N/A
Country(ies) of foreign collaborator:	N/A
Travelled to foreign country:	N/A
If traveled to foreign country(ies), duration of stay:	N/A

Name:	Daniele Fabris
Project Role:	Co-Principal Investigator
Nearest person month worked:	8
Contribution to Project:	No change
Funding Support:	None
Collaborated with individual in foreign country:	N/A
Country(ies) of foreign collaborator:	N/A
Travelled to foreign country:	N/A
If traveled to foreign country(ies), duration of stay:	N/A

Previously involved:

Name:	Crystal Huynh
Project Role:	Graduate Student
Nearest person month worked:	12
Contribution to Project:	No change
Funding Support:	None
Collaborated with individual in foreign country:	N/A
Country(ies) of foreign collaborator:	N/A
Travelled to foreign country:	N/A
If traveled to foreign country(ies), duration of stay:	N/A

Name:	Erica Brunelle
Project Role:	Graduate Student
Nearest person month worked:	30
Contribution to Project:	No change
Funding Support:	None
Collaborated with individual in foreign country:	N/A
Country(ies) of foreign collaborator:	N/A
Travelled to foreign country:	N/A
If traveled to foreign country(ies), duration of stay:	N/A

Other Collaborating Organizations

Nothing to report.

VII. REFERENCES

[1] Hair, M.; Mathis, A.; Brunelle, E.; Halamkova, L.; Halamek, J. *Anal. Chem.* **2018**, 17; 90 (8): 5322-5328.

[2] Finch, H. Comparison of Multivariate Means across Groups with Ordinal Dependent Variables: A Monte Carlo Simulation Study. *Front. Appl. Math. Stat.* **2016**, *2*. https://doi.org/10.3389/fams.2016.00002.

[3] Visualising associations between paired "omics" data sets. - PubMed - NCBI https://www.ncbi.nlm.nih.gov/pubmed/23148523 (accessed Feb 24, 2020).

[4] D.W. Foster, J.D. McGarry, The metabolic derangements and treatment of diabetic ketoacidosis, *N. Engl. J. Med.* 1983, 309 (3), 159-169.

[5] B. Persson, Determination of plasma acetoacetate and D-ß-hydroxy-butyrate in new-born infants by an enzymatic fluorometric micro-method, *Scand. J. Clin. Lab. Invest.* 1970, 25 (1), 9-18 (1970).

[6] K.E. Wildenhoff, A micro-method for the enzymatic determination of acetoacetate and 3-hydroxybutyrate in blood and urine, *Scand. J. Clin. Lab. Invest.* 1970, 25 (2), 171-179.

[7] D.D. Koch, H. Feidbruegge, Optimized kinetic method for automated determination of β-hydroxybutyrate, *Clin. Chem.* 1987, 33 (10), 1761-1766.

[8] Mitchell GA, Kassovska-Bratinova S, Boukaftane Y, Robert MF, Wang SP, Ashmarina L, Lambert M, Lapierre P, Potier E: Medical aspects of ketone body metabolism. *Clin Invest Med* **18**:193–216, 1995.

[9] Brunelle, E.; Huynh, C.; Le, A.−M.; Halamkova, L.; Agudelo, J.; Halamek, J. *Anal. Chem.* **2016**, 88, 2413−2420.

[10] Croxton, R. S.; Baron, M. G.; Butler, D.; Kent, T.; Sears, V. G. *Forensic Sci. Int.* **2010**, 199, 93−102.

[11] https://www.sigmaaldrich.com/catalog/product/sigma/n7285?lang=en&region=US

[12] Wu, Y.; Hussain, M.; Fassihi, R. *J. Pharmaceut. Biomed.* **2005**, 38, 263–269.

[13] Friedman, M. *J. Agric. Food Chem.*, **2004**, *52* (3), pp 385–406

[14] Brunelle, E.; Le, A.−M.; Huynh, C.; Wingfield, K.; Halamkova ,L.; Agudelo, J.; Halamek, J. *Anal. Chem.* **2017**, 89, 4314−4319.

[15] Compton, S. J.; Jones, C. G. *Anal. Biochem.* **1985**, 151, 369−374.

[16] http://www.bio-rad.com/featured/en/bradford-assay.html

[17] http://www.bio-rad.com/webroot/web/pdf/lsr/literature/4110065A.pdf

[18] https://www.thermofisher.com/order/catalog/product/23236

[19] https://www.brenda-enzymes.org/enzyme.php?ecno=1.1.1.30

[20] https://imagej.nih.gov/ij/docs/guide/146-30.html#toc-Subsection-30.7

[21] McGoldrick, L.; Weiss, E.; Halámek, J. Symmetric-key encryption based on bioaffinity interactions. *Synth. Bio. (ACS)* 2019, 8 (7):1655-1662.

[22] Koblitz, N. Cryptography as a Teaching Tool. *Cryptologia* **1997**. https://doi.org/10.1080/0161-119791885959.

[23] Sauerberg, J. From Private to Public Key Ciphers in Three Easy Steps http://www.mathaware.org/mam/06/Sauerberg_PKC-essay.html (accessed Nov 11, 2019).

[24] Jackson, W. An Introduction to the Android Studio Integrated Development Environment. *Android Apps Absol. Begin.* **2017**, 33–57. https://doi.org/10.1007/978-1-4842-2268-3_3.

[25] Ratner, B. The Correlation Coefficient: Its Values Range between +1/−1, or Do They? *J. Target. Meas. Anal. Mark.* **2009**, *17* (2), 139–142. https://doi.org/10.1057/jt.2009.5.

[26] W.N. Cumberland, Y. Fong, X. Yu, O. Defawe, N. Frahm, S. De Rosa. Nonlinear Calibration Model Choice between the Four and Five-Parameter Logistic Models. *Journal of Biopharmaceutical Statistics*, 25 (2015) 972–983.

[27] https://mycurvefit.com/

[28] K. Johnson. Curve Fitting for Immunoassays: ELISA and Multiplex Bead Based Assays (LEGENDplex™). BioLegend, Inc., 2019. Available from: https://www.biolegend.com/newsdetail/5468/

[29] TECHNICAL NOTE #2: Data Analysis for ELISA Assays. Biosensis Pty. Ltd., 2019. Available from: http://www.biosensis.com/documents/enhancedinfo/Technical-Note-2-ELISA-Data-Analysis.pdf